Adaptive Multiresolution Collocation Methods for Initial Boundary Value Problems of Nonlinear PDEs

Author(s): Wei Cai and Jianzhong Wang

Source: *SIAM Journal on Numerical Analysis*, Vol. 33, No. 3 (Jun., 1996), pp. 937-970
Published by: Society for Industrial and Applied Mathematics
Stable URL: http://www.jstor.org/stable/2158490
Accessed: 20-12-2017 20:48 UTC

SIAM J. NUMER. ANAL.
Vol. 33, No. 3, pp. 937-970, June 1996

006

ADAPTIVE MULTIRESOLUTION COLLOCATION METHODS FOR INITIAL BOUNDARY VALUE PROBLEMS OF NONLINEAR PDEs*

WEI CAI† AND JIANZHONG WANG‡

Abstract. We have designed a cubic spline wavelet-like decomposition for the Sobolev space $H_0^2(I)$ where I is a bounded interval. Based on a special point value vanishing property of the wavelet basis functions, a fast discrete wavelet transform (DWT) is constructed. This DWT will map discrete samples of a function to its wavelet expansion coefficients in at most $7N \log N$ operations. Using this transform, we propose a collocation method for the initial boundary value problem of nonlinear partial differential equations (PDEs). Then, we test the efficiency of the DWT and apply the collocation method to solve linear and nonlinear PDEs.

Key words. wavelet approximations, multiresolution analysis, fast discrete wavelet transform, collocation methods, IBV problems of PDEs

AMS subject classifications. Primary, 63N30, 65N13, 65F10; Secondary, 41A15, 42C05

1. Introduction.

Wavelet approximations have attracted much attention as a potentially efficient numerical technique for solving partial differential equations (PDEs) [1]-[6]. Because of their advantageous properties of localizations in both space and frequency domains [7]-[9], wavelets seem to be a great candidate for adaptive and multiresolution schemes to obtain solutions which vary dramatically both in space and time and develop singularities. However, to take advantage of the nice properties of wavelet approximations, we have to find an efficient way to deal with the nonlinearity and general boundary conditions in the PDEs. After all, most of the problems of fluid dynamics, which have solutions with quite different scales, are governed by nonlinear PDEs with complicated boundary conditions. Therefore, it is our objective here to address these issues when designing wavelet numerical schemes for nonlinear PDEs.

Most of the wavelet approximation schemes for PDEs so far have been based on the wavelet decomposition of $L^2(R)$ with Daubechies' orthonormal wavelets on the whole real line R (see [1]-[6]). However, in solving the initial boundary value problem, treatment of the boundary conditions is an important aspect of any numerical scheme. In [1] an embedded domain approach is used so that the boundary condition gets absorbed into the PDEs via a penalty term. In [6], by using the primitive function of Daubechies' wavelet and its dilations and translations, the authors construct a Riesz basis for the Sobolev space $H_0^1(I)$ defined on a bounded interval I. Another common way to achieve wavelet approximation on a bounded interval is to keep all Daubechies' wavelets (or compactly supported spline wavelets), whose supports are totally inside the interval, intact while modifying those wavelets intersecting the boundary by an orthonormalization (semiorthogonalization) procedure (see [10]-[12]).

However, we believe that a more natural approach for approximating a PDE's solution in a Sobolev space $H_0^2(I)$ is to construct directly a multiresolution analysis (MRA) ($V_0 \subset V_1 \subset V_2 \cdots$) for $H_0^2(I)$ where V_j is generated by some scaling functions through dilations and translations. Using such an MRA, we can decompose $H_0^2(I)$ into the form $H_0^2(I) = V_0 \oplus_{j=0}^{\infty} W_j$, where $\oplus$ stands for orthogonal direct sum and W_j denotes the orthogonal compliment of V_j

*Received by the editors July 21, 1994; accepted for publication (in revised form) July 22, 1994. This research was supported by National Science Foundation grant ASC-9113895 and Air Force Office of Scientific Research grant F49620-94-1-0317.

†Department of Mathematics, University of California, Santa Barbara, CA 93106 (wcai@uncc.edu). This author received a supercomputing grant from the North Carolina Supercomputer Center and was partially supported by National Aeronautics and Space Administration contract NAS1-19480 while he was in residence at the Institute for Computer Applications in Science and Engineering (ICASE), National Aeronautics and Space Administration, Langley Research Center, Hampton, VA 23681-0001.

‡Department of Mathematics, Sam Houston State University, Huntsville, TX 77341. This author is supported by National Science Foundation grant DMS-9503282.

in the space V_{j+1}: $V_{j+1} = V_j \oplus W_j$. Then we show that the basis of all the subspaces W_j can be essentially generated from one function ("mother wavelet") by dilations and translations except the two boundary functions in each W_j which are generated from another function located at the boundary ("mother boundary wavelet") by dilations and reflections. Because the inner product considered here is in space $H_0^2(I)$, not in space $L^2(I)$, these two mother wavelet functions will no longer have vanishing moments of the first two orders as usual wavelets in space L^2 (see (3.17)). For simplicity, we will still use the term "wavelet" throughout this paper with the understanding that it is different from the usual wavelet with its nonvanishing moment. It is worthwhile to point out that despite the fact that these wavelet-like functions have no vanishing moments, the projection f_j of any function $f \in H_0^2(I)$ on V_j still provides a "blurred" version of function f while the one on space W_j keeps its local details. Hence the magnitude of coefficients in the wavelet expansion of functions in $H_0^2(I)$ does reflect the local scales and changes of the function to be approximated. It is these features that are needed for achieving adaptivities and MRAs in practical computations. Here we would like to mention Harten's recent work [13], his approach for designing a scheme for multiresolution representation of numerical data without directly using the wavelet idea is successfully applied in reducing the computational costs of numerical fluxes in Godunov schemes for shock-wave computations.

To design a wavelet collocation method for nonlinear time evolution problems, the key point is to construct a discrete wavelet transform (DWT) which maps between function values and the wavelet coefficient space such that the resulting wavelet expansion interpolates the function values. In this paper, we will use a cubic spline wavelet basis of $H_0^2(I)$ [14] for the construction of a DWT. A special point value vanishing property (see (3.7)) of this wavelet basis results in $O(N \log N)$ operations for the DWT where N is the total number of unknowns. Therefore, the nonlinear term in the PDE can be easily treated in the physical space and the derivatives of those nonlinear terms can be computed in the wavelet space. As a result, collocation methods will provide the flexibility of handling nonlinearity and various boundary conditions. In [15], a different method based on scale separation was suggested to compute the wavelet approximation of $f(u)$ given a wavelet expansion with Daubechies' wavelets for u.

The rest of this paper is divided into the following six sections. In §2, we introduce the cubic scaling functions $\phi(x)$, $\phi_b(x)$ and their wavelet functions $\psi(x)$, $\psi_b(x)$. An MRA and its corresponding wavelet decomposition of the Sobolev space $H_0^2(I)$ are constructed using $\phi(x)$, $\phi_b(x)$ and $\psi(x)$, $\psi_b(x)$. Then, we show how to construct a wavelet approximation for functions in the Sobolev space $H^2(I)$. In §3, we introduce the fast DWT between functions and their wavelet coefficients. In §4, we discuss the derivative matrix $\mathcal{D}$ for approximating differential operators. In §5, we present the wavelet collocation methods for nonlinear time evolution PDEs. In §6, we give the central processing unit (CPU) time performance of the DWTs and the numerical results of the wavelet collocation methods for linear and nonlinear PDEs. A conclusion is given in §7.

2. Scaling functions $\phi(x)$, $\phi_b(x)$ and wavelet functions $\psi(x)$, $\psi_b(x)$. Let I denote a finite interval, say $I = [0, L]$, L be a positive integer (for the sake of simplicity, we assume that $L > 4$), and $H^2(I)$ and $H_0^2(I)$ denote the following two Sobolev spaces:

$$H^2(I) = \{f(x), x \in I \mid \|f^{(i)}\|_2 < \infty, i = 0, 1, 2\}, \tag{2.1}$$

$$H_0^2(I) = \{f(x) \in H^2(I) \mid f(0) = f'(0) = f(L) = f'(L) = 0\}. \tag{2.2}$$

It can be easily checked [16] that $H_0^2(I)$ is a Hilbert space equipped with inner product

$$\langle f, g \rangle = \int_I f''(x) g''(x)\, dx, \tag{2.3}$$

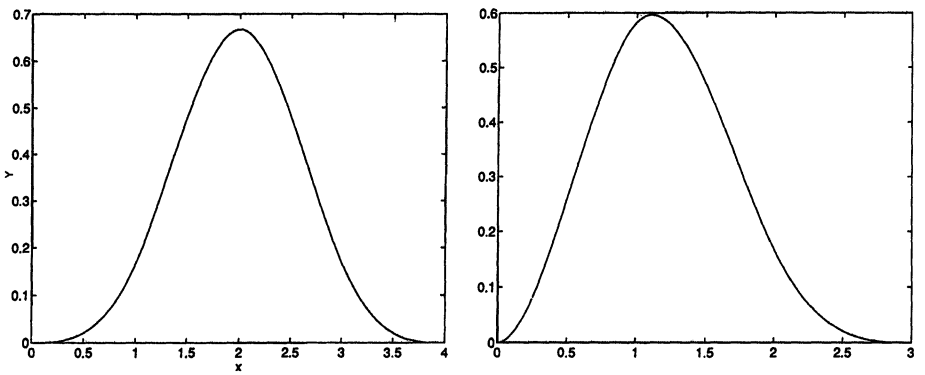

FIG. 1. *Interior scaling functions* $\phi(x)$ (a) *and boundary scaling function* $\phi_b(x)$.

thus,

$$|||f||| = \sqrt{\langle f, f\rangle} \tag{2.4}$$

provides a norm for $H_0^2(I)$.

To generate an MRA for the Sobolev space $H_0^2(I)$, we consider two scaling functions; specifically, we consider an interior scaling function $\phi(x)$ and a boundary scaling function $\phi_b(x)$ (see Figure 1):

$$\phi(x) = N_4(x) = \frac{1}{6}\sum_{j=0}^{4}\binom{4}{j}(-1)^j(x-j)_+^3, \tag{2.5}$$

$$\phi_b(x) = \frac{3}{2}x_+^2 - \frac{11}{12}x_+^3 + \frac{3}{2}(x-1)_+^3 - \frac{3}{4}(x-2)_+^3, \tag{2.6}$$

where $N_4(x)$ is the fourth-order B-spline [17] and for any real number n

$$x_+^n = \begin{cases} x^n & \text{if } x \geq 0, \\ 0 & \text{otherwise.} \end{cases}$$

As a pair they satisfy the two-scale relationships given in Lemma 1.

LEMMA 1.

$$\phi(x) = \sum_{k=0}^{4} 2^{-3}\binom{4}{k}\phi(2x-k),$$

$$\phi_b(x) = \beta_{-1}\phi_b(2x) + \sum_{k=0}^{2}\beta_k\phi(2x-k), \tag{2.7}$$

$$\textit{where}\quad \beta_{-1} = \frac{1}{4}, \beta_0 = \frac{11}{16}, \beta_1 = \frac{1}{2}, \beta_2 = \frac{1}{8}.$$

We summarize some properties of $\phi(x)$ and $\phi_b(x)$ in the following lemma.

LEMMA 2. *Let* $\phi(x)$ *and* $\phi_b(x)$ *be defined as in* (2.5) *and* (2.6). *Then we have*

(2.8) (1) $\text{supp}(\phi(x)) = [0, 4]$;

(2.9) (2) $\text{supp}(\phi_b(x)) = [0, 3]$;

(2.10) (3) $\phi(x), \phi_b(x) \in H_0^2(I)$;

(2.11) (4) $\phi'(1) = -\phi'(3) = \frac{1}{2},\ \phi'(2) = 0,\ \phi_b'(1) = \frac{1}{4}, \phi_b'(2) = -\frac{1}{2}$;

(2.12) (5) $\phi(1) = \phi(3) = \frac{1}{6},\ \phi(2) = \frac{2}{3},\ \phi_b(1) = \frac{7}{12},\ \phi_b(2) = \frac{1}{6}$.

For any $j, k \in Z$, we define

(2.13) $$\phi_{j,k}(x) = \phi(2^j x - k), \qquad \phi_{b,j}(x) = \phi_b(2^j x),$$

and let V_j be the linear span of $\{\phi_{j,k}(x), 0 \le k \le 2^j L - 4, \phi_{b,j}(x), \phi_{b,j}(L-x)\}$, namely,

(2.14) $$V_j = span\{\phi_{j,k}(x) \mid 0 \le k \le 2^j L - 4; \phi_{b,j}(x), \phi_{b,j}(L-x)\}.$$

THEOREM 1. *Let V_j, $j \in \mathbf{Z}^+$ be the linear span of* (2.14). *Then V_j forms an MRA for $H_0^2(I)$ equipped with norm* (2.4) *in the following sense:*

(i) $V_0 \subset V_1 \subset V_2 \subset \cdots$;

(ii) $clos_{H_0^2}(\bigcup_{j\in\mathbf{Z}^+} V_j) = H_0^2(I)$;

(iii) $\bigcap_{j\in\mathbf{Z}^+} V_j = V_0$; *and*

(iv) *for each j, $\{\phi_{j,k}(x), \phi_{b,j}(x), \phi_{b,j}(L-x)\}$ is a basis of V_j.*

Proof. The proofs for (iii) and (iv) are straightforward and omitted here. The proof for (i) follows from (2.7) in Lemma 1. To prove (ii), we recall some familiar results on interpolating cubic splines for smooth functions [18], [19].

LEMMA 3. *Let π be the partition given by $x_i = ih$, $0 \le i \le n$, $h = \frac{(b-a)}{n}$, and $s(x)$ be the cubic spline interpolating $f(x) \in C^4[a, b]$ at all points in π, i.e.,*

$$s(x_i) = f(x_i), \qquad 0 \le i \le n,$$

and satisfying the following boundary conditions:

(2.15) $$s'(a) = f'(a), \qquad s'(b) = f'(b).$$

Then

1. *$s(x)$ uniquely exists and*

(2.16) $$||s^{(r)} - f^{(r)}||_\infty \le \epsilon_r ||f^{(4)}||_\infty h^{4-r}, \qquad r = 0, 1, 2, 3,$$

where $\epsilon_0 = \frac{5}{384}, \epsilon_1 = \frac{1}{24}, \epsilon_2 = \frac{3}{8}, \epsilon_3 = 1$;

2. *if the average operator R is defined by*

(2.17) $$R(s'')(x_i) = \frac{s''(x_{i-1}) + 10s''(x_i) + s''(x_{i+1})}{12} \quad \text{for } 1 \le i \le n-1,$$

then

(2.18) $$R(s'')(x_i) - f''(x_i) = O(h^4).$$

Proof of (ii) *of Theorem* 1. Let $h = \frac{1}{2^j}$, $a = 0$, and $b = L$. Consider $f(x) \in C_0^\infty(0, L)$. Since $C_0^\infty(0, L) \subset C^4[0, L] \cap H_0^2(0, L)$, by Lemma 3, there is a unique cubic spline corresponding to the partition π interpolating $f(x)$. From the fact that $f(0) = f(L) = f'(0) = f'(L) = 0$, we have $s(x)$ in V_j and then

(2.19) $$s(x) = c_{-1}\phi_{b,j}(x) + \sum_{k=0}^{n_j-4} c_k \phi_{j,k}(x) + c_{L-3}\phi_{b,j}(L-x)$$

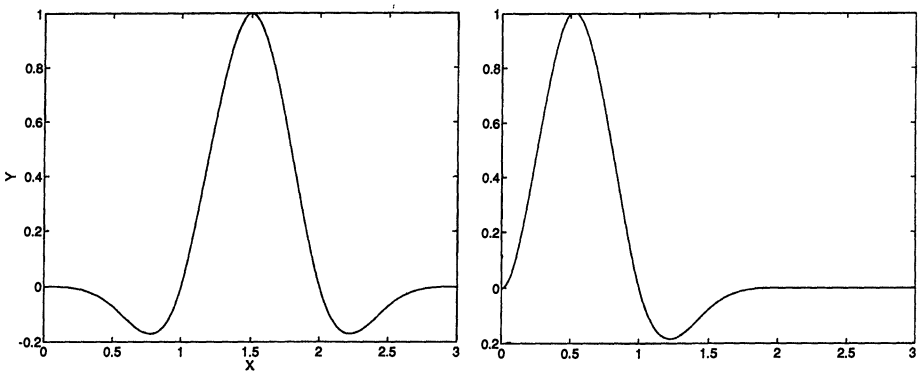

FIG. 2. *Interior wavelet functions* $\psi(x)$ (a) *and boundary wavelet function* $\psi_b(x)$.

such that

$$s(x_i) = f(x_i), \qquad 0 \le i \le n_j, \tag{2.20}$$

where $n_j = 2^j L$, $x_i = \frac{i}{n_j} L$.

Finally, from (2.16) in Lemma 3 with $r = 2$ we have

$$|||s - f||| = ||s^{(2)} - f^{(2)}||_{L^2} \le L||s^{(2)} - f^{(2)}||_\infty \le \epsilon_2 L 2^{-2j}||f^{(4)}||_\infty.$$

Therefore, as $j \longrightarrow \infty$, $|||s - f||| \longrightarrow 0$. This proves that $C_0^\infty(0, L) \subset clos_{H_0^2}(\bigcup_{j\in Z^+} V_j)$.

Thus, Theorem 1(ii) follows from the fact that $C_0^\infty(0, L)$ is dense in $H_0^2(0, L)$. □

To construct a wavelet decomposition of Sobolev space $H_0^2(I)$ under the inner product (2.3), we consider the following two wavelet functions $\psi(x)$, $\psi_b(x)$ (see Figure 2):

$$\psi(x) = -\frac{3}{7}\phi(2x) + \frac{12}{7}\phi(2x-1) - \frac{3}{7}\phi(2x-2) \in V_1, \tag{2.21}$$

$$\psi_b(x) = \frac{24}{13}\phi_b(2x) - \frac{6}{13}\phi(2x) \in V_1. \tag{2.22}$$

It can be verified that $\psi(x)$ and $\psi_b(x)$ both belong to V_1 and

$$\psi(n) = \psi_b(n) = 0 \quad \text{for all } n \in Z. \tag{2.23}$$

Property (2.23) will be important in the construction of a fast DWT later. Now we define

$$\psi_{j,k}(x) = \psi(2^j x - k), \qquad j \ge 0,\ k = 0, \ldots, n_j - 3, \tag{2.24}$$

$$\psi^l_{b,j}(x) = \psi_b(2^j x), \qquad \psi^r_{b,j}(x) = \psi_b(2^j(L - x)), \tag{2.25}$$

where again $n_j = 2^j L$. For the sake of simplicity, we will adopt the following notation:

$$\psi_{j,-1}(x) = \psi^l_{b,j}(x), \qquad \psi_{j,n_j-2}(x) = \psi^r_{b,j}(x). \tag{2.26}$$

So, when $k = -1$ and $n_j - 2$, wavelet functions $\psi_{j,k}(x)$ will denote the two boundary wavelet functions, which cannot be obtained by translating and dilating $\psi(x)$.

Finally, for each $j \ge 0$, we define

$$W_j = span\{\psi_{j,k}(x) \mid k = -1, \ldots, n_j - 2\}. \tag{2.27}$$

THEOREM 2. *The W_j, $j \geq 0$, defined in* (2.27) *is the orthogonal compliment of V_j in V_{j+1} under the inner product* (2.3), *i.e.,*

(1) *$V_{j+1} = V_j \oplus W_j$ for $j \in \mathbf{Z}^+$, where $\oplus$ stands for $V_j \perp W_j$ under the inner product* (2.3) *and $V_{j+1} = V_j + W_j$. Therefore,*

(2) *$W_j \perp W_{j+1}$, $j \in \mathbf{Z}^+$, and*

(3) *$H_0^2(I) = V_0 \oplus_{j \in \mathbf{Z}^+} W_j$.*

Proof. (1) We only have to prove $V_j \oplus W_j$ for $j = 0$, namely, for $0 \leq l \leq L-4$, $0 \leq k \leq L-3$,

$$\langle \phi(x-l), \psi(x-k) \rangle = 0, \tag{2.28}$$

$$\langle \phi(x-l), \psi_b(x) \rangle = 0, \tag{2.29}$$

$$\langle \phi_b(x), \psi(x-k) \rangle = 0, \tag{2.30}$$

$$\langle \phi_b(x), \psi_b(x) \rangle = 0. \tag{2.31}$$

Integrating by parts twice in (2.28) and using the fact that $\psi(x), \phi(x) \in H_0^2(I)$, we have

$$\begin{aligned}
\langle \phi(x-l), \psi(x-k) \rangle &= \int_0^L \phi''(x-l)\psi''(x-k)\,dx \\
&= \phi''(x-l)\psi'(x-k)|_0^L - \int_0^L \phi^{(3)}(x-l)\psi'(x-k)\,dx \\
&= -\int_0^L \phi^{(3)}(x-l)\psi'(x-k)\,dx \\
&= -\phi^{(3)}(x-l)\psi(x-k)|_0^L + \int_0^L \phi^{(4)}(x-l)\psi(x-k)\,dx \\
&= \int_0^L \phi^{(4)}(x-l)\psi(x-k)\,dx.
\end{aligned}$$

From equation (2.23) and an easily checked identity,

$$\phi^{(4)}(x) = \sum_{j=0}^{4} \binom{4}{j} (-1)^j \delta(x-j),$$

where $\delta(x)$ is the Dirac-delta function. So we have

$$\langle \phi(x-l), \psi(x-k) \rangle = \sum_{j=0}^{4} \binom{4}{j} (-1)^j \psi(j-(k-l)) = 0.$$

Equations (2.29)–(2.31) can be shown in a similar way. So (1) follows from (2.21) and (2.22) and the fact that $\dim V_j = 2^j L - 1$ and $\dim W_j = 2^j L$, and then $\dim V_{j+1} = 2^{j+1}L - 1 = (2^j L - 1) + 2^j L = \dim V_j + \dim W_j$; (2) follows from (1); and (3) follows directly from Theorem 1 (ii). □

As a consequence of Theorem 2, any function $f(x) \in H_0^2(I)$ can be approximated as closely as needed by a function $f_j(x) \in V_j = V_0 \oplus W_0 \oplus W_1 \oplus \cdots \oplus W_{j-1}$ for a sufficiently large j, and $f_j(x)$ has a unique orthogonal decomposition

$$f_j(x) = f_0 + g_0 + g_1 + \cdots + g_{j-1}, \tag{2.32}$$

where $f_0 \in V_0$, $g_i \in W_i$, $0 \leq i \leq j-1$.

2.1. Approximation for a function in $H^2(I)$. Consider the following two splines:

$$\eta_1(x) = (1-x)_+^3, \tag{2.33}$$

$$\eta_2(x) = 2x_+ - 3x_+^2 + \frac{7}{6}x_+^3 - \frac{4}{3}(x-1)_+^3 + \frac{1}{6}(x-2)_+^3. \tag{2.34}$$

For any function $f(x) \in H^2(I)$, we have $f(x) \in C^1(I)$, by the Sobolev embedding theorem. Therefore, we can define the following interpolating spline $\mathbf{I}_{b,j} f(x)$, $j \geq 0$:

$$\mathbf{I}_{b,j} f(x) = \alpha_1 \eta_1(2^j x) + \alpha_2 \eta_2(2^j x) + \alpha_3 \eta_2(2^j(L-x)) + \alpha_4 \eta_1(2^j(L-x)), \tag{2.35}$$

where the coefficients $\alpha_1, \alpha_2, \alpha_3, \alpha_4$ are determined by certain interpolating conditions we will state below. Since spline $\mathbf{I}_{b,j} f(x)$ is expected to approximate the nonhomogeneities of function $f(x)$ at the boundaries, these interpolating conditions will also be called end conditions. The following two kinds of end conditions are common in applications.

2.1.1. Derivative end conditions. We can impose the following end-derivative conditions:

$$\mathbf{I}_{b,j} f(0) = f(0), \qquad \mathbf{I}_{b,j} f(L) = f(L), \tag{2.36}$$

$$(\mathbf{I}_{b,j} f)'(0) = f'(0), \qquad (\mathbf{I}_{b,j} f)'(L) = f'(L). \tag{2.37}$$

It can be easily verified that if we choose

$$\alpha_1 = f(0), \qquad \alpha_2 = \frac{f'(0)}{2^{j+1}} + \frac{3}{2} f(0) \tag{2.38}$$

$$\alpha_3 = -\frac{f'(L)}{2^{j+1}} + \frac{3}{2} f(L), \qquad \alpha_4 = f(L),$$

then $I_{b,j} f$ satisfies conditions (2.36), (2.37).

In many situations, however, we do not know the values of derivatives $f'(0)$, $f'(L)$. Then they have to be approximated by finite differences using only the values of $f(x)$. To preserve the exact order of accuracy for the cubic spline approximation, we suggest using the following approximations:

$$f'(0) = \frac{1}{h} \sum_{k=0}^{p} c_k f(kh) + O(h^s), \tag{2.39}$$

$$f'(L) = -\frac{1}{h} \sum_{k=0}^{p} c_k f(L-kh) + O(h^s),$$

where $h > 0$ and $p \geq 3$. For $p = 3$, if we take

$$c_0 = -\frac{11}{6}, \qquad c_1 = 3, \qquad c_2 = -\frac{3}{2}, \qquad c_3 = \frac{1}{3},$$

then $s = 3$ in (2.39), and thus, equation (2.37) is satisfied within an error of $O(h^3)$. Correspondingly, the coefficients α_k, $1 \leq k \leq 4$, for $\mathbf{I}_{b,j} f(x)$ become

$$\alpha_1 = f(0), \qquad \alpha_2 = \sum_{k=0}^{p} c_k' f(kh), \tag{2.40}$$

$$\alpha_3 = \sum_{k=0}^{p} c_k' f(L-kh), \qquad \alpha_4 = f(L),$$

where

$$c_0' = \left(\frac{1}{2^{j+1}h}c_0 + \frac{3}{2}\right), \qquad c_k' = \frac{c_k}{2^{j+1}h}, \quad 1 \le k \le p.$$

Now we have $f(x) - \mathbf{I}_{b,j}f(x) \in H_0^2(I)$ and the decomposition (2.32) can be applied. Finally, for any function $f(x) \in H^2(I)$, we can find a function $f_j(x)$ in the form of

$$f_j(x) = \mathbf{I}_{b,j}f + f_0 + g_0 + g_1 + \cdots + g_{j-1}, \qquad f_0 \in V_0,\ g_i \in W_i,\ 0 \le i \le j-1, \tag{2.41}$$

which approximates $f(x)$ as closely as needed provided that j is large enough. Furthermore, by Lemma 3, the approximation order will be $O(2^{-4j})$ if $f_j(x)$ is chosen as the interpolating spline of $f(x)$.

2.1.2. Not-a-knot conditions. In many applications, the solutions vary dramatically near the boundary, so approximation (2.39) to the end derivatives could result in large errors. In those cases, we prefer to use the so-called not-a-knot end conditions [20], which amounts to requiring that the spline $I_{b,j}f(x)$ agrees with function $f(x)$ at one additional point near each boundary. So we have the following equations for α_k, $1 \le k \le 4$:

$$\begin{aligned} \mathbf{I}_{b,j}f(0) &= f(0), \qquad \mathbf{I}_{b,j}f(L) = f(L), \\ \mathbf{I}_{b,j}f(\tau_1) &= f(\tau_1), \qquad \mathbf{I}_{b,j}f(\tau_2) = f(\tau_2). \end{aligned} \tag{2.42}$$

In our case, by choosing $\tau_1 = \frac{1}{2^{j+1}}$, $\tau_2 = L - \frac{1}{2^{j+1}}$, we have

$$\begin{aligned} \alpha_1 &= f(0), \qquad \alpha_2 = 6f(\tau_1) - \frac{3f(0)}{4}, \\ \alpha_3 &= 6f(\tau_2) - \frac{3f(L)}{4}, \qquad \alpha_4 = f(L). \end{aligned} \tag{2.43}$$

Although in this case $f(x) - \mathbf{I}_{b,j}f(x)$ is no longer in the space $H_0^2(I)$, an interpolating spline $f_j(x)$ in the form of (2.41) with $I_{b,j}f(x)$ defined in (2.42) will still have an approximation to $f(x)$ of order $O(2^{-4j})$ [21].

3. DWT. In this section, we will introduce a fast DWT which maps discrete sample values of a function to its wavelet interpolant expansions. Such expansion with the wavelet decomposition will enable us to compute an approximation of the first and second derivatives of the function.

3.1. Interpolant operator $\mathbf{I}_{V0}$ in V_0. Consider any function $f(x) \in H_0^2(I)$ and denote the interior knots for V_0 by

$$x_k^{(-1)} = k, \qquad k = 1, \ldots, L-1 \tag{3.1}$$

and the values of $f(x)$ on $\{x_k^{(-1)}\}_{k=1}^{L-1}$ by

$$f_k^{(-1)} = f(x_k^{(-1)}), \qquad k = 1, \ldots, L-1. \tag{3.2}$$

The cubic interpolant $\mathbf{I}_{V0}f(x)$ of data $\{f_k^{(-1)}\}$ can be expressed as

$$\mathbf{I}_{V0}f(x) = c_{-1}\phi_b(x) + \sum_{k=0}^{L-4} c_k\phi_{0,k}(x) + c_{L-3}\phi_b(L-x) \tag{3.3}$$

and $\mathbf{I}_{V0}f(x)$ interpolates data $f_k^{(-1)}$, $k = 1, \ldots, L-1$, namely,

$$\mathbf{I}_{V0}f(x_k^{(-1)}) = f_k^{(-1)}, \qquad k = 1, \ldots, L-1. \tag{3.4}$$

Let $\mathbf{B}$ be the transform matrix between $\mathbf{f}^{(-1)} = (f_1^{(-1)}, \ldots, f_{L-1}^{(-1)})^\top$ and the coefficient $\mathbf{c} = (c_{-1}, \ldots, c_{L-3})^\top$, i.e.,

$$\mathbf{f}^{(-1)} = \mathbf{B}\mathbf{c}, \tag{3.5}$$

where by using item (5) in Lemma 2, we have

$$\mathbf{B} = \begin{pmatrix} \frac{7}{12} & \frac{1}{6} & & & & & & \\ \frac{1}{6} & \frac{2}{3} & \frac{1}{6} & & & & & \\ & \frac{1}{6} & \frac{2}{3} & \frac{1}{6} & & & & \\ & & \ddots & \ddots & \ddots & & & \\ & & & \frac{1}{6} & \frac{2}{3} & \frac{1}{6} & & \\ & & & & \frac{1}{6} & \frac{2}{3} & \frac{1}{6} & \\ & & & & & \frac{1}{6} & \frac{7}{12} \end{pmatrix}$$

To obtain the coefficients c_k, $-1 \le k \le L-3$, in (3.3), we have to solve the tridiagonal system (3.5), which involves $(8L)$ operations.

3.2. Interpolation operator $\mathbf{I}_{W_j}f$ in W_j. Similarly, we can define the interpolation operator $\mathbf{I}_{W_j}f(x)$ in W_j, $j \ge 0$, for any function $f(x)$ in $H_0^2(I)$. For this purpose, we choose the following interpolation points in I:

$$x_k^{(j)} = \frac{k+1.5}{2^j}, \qquad -1 \le k \le n_j - 2, \tag{3.6}$$

where $n_j = \mathrm{Dim}W_j = 2^j L$.

It can be checked that for the interpolation points $\{x_k^{(-1)}\}$ for V_0 in (3.1) and $\{x_k^{(j)}\}$ for W_j, $j \ge 0$, in (3.6), the wavelet functions $\psi_{j,k}(x)$ satisfy a point value vanishing property.

3.2.1. Point value vanishing property of $\psi_{j,k}(x)$. For $j > i$, $-1 \le k \le n_j - 2$,

$$\begin{aligned} &\psi_{j,k}(x_k^{(j)}) = 1, \\ &\psi_{j,k}(x_l^{(i)}) = 0, \qquad -1 \le \ell \le n_i - 2, \text{ if } i \ge 0;\ 1 \le \ell \le L-1, \text{ if } i = -1. \end{aligned} \tag{3.7}$$

So $\{\phi_{0,k}(x)\}, \{\psi_{j,k}(x)\}_{j=0}^{\infty}$ form a hierarchical basis for the Sobolev space $H_0^2(I)$ [22]. Moreover, the point value vanishing property will be crucial in obtaining a fast DWT.

The interpolation $\mathbf{I}_{W_j}f(x)$ of a function $f(x) \in H_0^2(I)$ in W_j, $j \ge 0$, can be expressed as a linear combination of $\psi_{j,k}(x)$, $k = -1, \ldots, n_j - 2$, namely,

$$\mathbf{I}_{W_j}f(x) = \sum_{k=-1}^{n_j-2} \hat{f}_{j,k}\psi_{j,k}(x) \tag{3.8}$$

and

$$\mathbf{I}_{W_j}f(x_k^{(j)}) = f(x_k^{(j)}), \qquad -1 \le k \le n_j - 2.$$

If we denote $\mathbf{M}_j$ as the n_jth-order matrix that relates $\hat{\mathbf{f}}^{(j)} = (\hat{f}_{j,-1}, \ldots, \hat{f}_{j,n_j-2})^\top$ and $\mathbf{f}^{(j)} = (f(x_{-1}^{(j)}), \ldots, f(x_{n_j-2}^{(j)}))^\top$, then

$$\mathbf{f}^{(j)} = \mathbf{M}_j \hat{\mathbf{f}}^{(j)}, \tag{3.9}$$

where

$$\mathbf{M}_j = \begin{pmatrix} 1 & -\frac{1}{14} & & & & & & \\ -\frac{1}{13} & 1 & -\frac{1}{14} & & & & & \\ & -\frac{1}{14} & 1 & -\frac{1}{14} & & & & \\ & & \ddots & \ddots & \ddots & & & \\ & & & -\frac{1}{14} & 1 & -\frac{1}{14} & & \\ & & & & -\frac{1}{14} & 1 & -\frac{1}{13} & \\ & & & & & -\frac{1}{14} & 1 & \end{pmatrix}.$$

The solution of the coefficients $\{\hat{f}_{j,k}, -1 \le k \le n_j - 2\}$ again involves solving a tridiagonal system (3.9) which costs $(8n_j)$ operations.

Now let us assume that the values of a function $f(x) \in H_0^2(I)$ are given on all the interpolation points $\{x_k^{(j)}\}$ defined in (3.1) and (3.6). We intend to find the wavelet interpolation $\mathcal{P}_J f(x) \in V_0 \oplus W_0 \oplus W_1 \oplus \cdots \oplus W_{J-1}$ for $J - 1 \ge 0$, i.e.,

$$\begin{aligned} \mathcal{P}_J f(x) &= \hat{f}_{-1,-1}\phi_b(x) + \sum_{k=0}^{L-4} \hat{f}_{-1,k}\phi_k(x) + \hat{f}_{-1,L-3}\phi_b(L-x) \\ &\quad + \sum_{j=0}^{J-1} \left[\sum_{k=-1}^{n_j-2} \hat{f}_{j,k}\psi_{j,k}(x) \right] \\ &= f_{-1}(x) + \sum_{j=0}^{J-1} f_j(x), \end{aligned} \tag{3.10}$$

where

$$f_{-1}(x) = \mathbf{I}_{V0} f(x) \in V_0, \qquad f_j(x) = \sum_{k=-1}^{n_j-2} \hat{f}_{j,k}\psi_{j,k}(x) \in W_j, \quad j \ge 0,$$

and the following interpolating conditions hold:

$$\begin{aligned} \mathcal{P}_J f(x_k^{(-1)}) &= f(x_k^{(-1)}), \qquad 1 \le k \le L-1, \\ \mathcal{P}_J f(x_k^{(j)}) &= f(x_k^{(j)}), \qquad j \ge 0, -1 \le k \le n_j - 2. \end{aligned} \tag{3.11}$$

Let us denote by $\mathbf{f} = (\mathbf{f}^{(-1)}, \mathbf{f}^{(0)}, \ldots, \mathbf{f}^{(J-1)})^\top$ the values of $f(x)$ on all interpolation points, i.e.,

$$\begin{aligned} \mathbf{f}^{(-1)} &= \{f(x_k^{(-1)})\}_{k=1}^{L-1}, \\ \mathbf{f}^{(j)} &= \{f(x_k^{(j)})\}_{k=-1}^{n_j-2}, \qquad j \ge 0, \end{aligned}$$

and by $\hat{\mathbf{f}} = (\hat{\mathbf{f}}^{(-1)}, \hat{\mathbf{f}}^{(0)}, \ldots, \hat{\mathbf{f}}^{(J-1)})^\top$ the wavelet coefficients in the expansion (3.10):

$$\begin{aligned} \hat{\mathbf{f}}^{(-1)} &= \{\hat{f}_{-1,k}\}_{k=1}^{L-1}, \\ \hat{\mathbf{f}}^{(j)} &= \{\hat{f}_{j,k}\}_{k=-1}^{n_j-2}, \qquad j \ge 0. \end{aligned}$$

The following algorithm provides a recursive way to compute all the wavelet coefficients $\hat{\mathbf{f}}$. Note that the wavelet expansion (3.10) can be expanded to include higher-level wavelet spaces W_j, $J \le j \le J'$, by adding only terms from the higher wavelet spaces, i.e., $W_J, \ldots, W_{J'-1}$.

3.3. DWT for $\hat{\mathbf{f}} \longrightarrow \mathbf{f}$. This direction of transform is straightforward by evaluating the expansion (3.10) at all the collocation points $\{x_k^{(j)}\}$, $j \ge -1$. The point value vanishing property (3.7) of the wavelet functions and the compactness of $\mathrm{supp}\psi_{j,k}(x)$ can be used to reduce the number of evaluations.

Number of operations. Let N be the total number of collocation points and $N = (L-1) + \sum_{j=0}^{J-1} n_j = 2^J L - 1$. In the evaluation of $\mathcal{P}_J f(x_k^{(j)})$, values of $\psi(x)$ and $\phi(x)$ at dyadic points $\frac{k}{2^J}$ are needed and they can be computed once for future use.

Recalling (3.10) and the point value vanishing property (3.7) of the wavelet basis functions, we have

$$\mathcal{P}_J f(x_k^{(-1)}) = f_{-1}(x_k^{(-1)}), \qquad 1 \le k \le L-1,$$

which needs $4(L-1)$ (flops).

For each $0 \le j \le J-1$, to compute $\mathcal{P}_J f(x_k^{(j)})$, $-1 \le k \le n_j - 2$, requires $5jn_j$ (flops). Thus, it takes $4(L-1) + \sum_{j=0}^{J-1} 5jn_j \le 5N \log N$ (flops) to compute the vector $\mathbf{f}$.

3.4. DWT for $\mathbf{f} \longrightarrow \hat{\mathbf{f}}$. Recalling that $\mathbf{f} = (\mathbf{f}^{(-1)}, \mathbf{f}^{(0)}, \ldots, \mathbf{f}^{(J-1)})^\top$, we proceed to the construction of $\mathcal{P}_J f(x)$ in the following steps.

Step 1. Define

$$f_{-1}(x) = \mathbf{I}_{V0}\mathbf{f}^{(-1)} = \hat{f}_{-1,-1}\phi_b(x) + \sum_{k=0}^{L-4} \hat{f}_{-1,k}\phi_k(x) + \hat{f}_{-1,L-3}\phi_b(L-x),$$

so $f_{-1}(x)$ interpolates $f(x)$ at the interpolation points $x_k^{(-1)}$, $-1 \le k \le L-1$, namely,

$$f_{-1}(x_k^{(-1)}) = f(x_k^{(-1)}). \tag{3.12}$$

Step 2. Define

$$f_0(x) = \mathbf{I}_{W_0}(\mathbf{f}^{(0)} - (\mathbf{I}_{V0}f)^{(0)}) = \sum_{l=-1}^{n_0-2} \hat{f}_{0,l}\psi_{0,l}(x), \tag{3.13}$$

where $(\mathbf{I}_{V0}f)^{(0)} = \{\mathbf{I}_{V0}f(x_k^{(0)})\}_{k=-1}^{n_0-2}$.

As a result of the, point value vanishing property (3.7) of the wavelet functions, we have $\psi_{0,l}(x_k^{(-1)}) = 0$, $-1 \le l \le n_0 - 2$, $1 \le k \le L-1$, thus

$$f_0(x_k^{(-1)}) = 0, \qquad 1 \le k \le L-1.$$

So we have, for $1 \le k \le L-1$,

$$\begin{aligned} f_{-1}(x_k^{(-1)}) + f_0(x_k^{(-1)}) &= f_{-1}(x_k^{(-1)}) = \mathbf{I}_{V0}f(x_k^{(-1)}) = f(x_k^{(-1)}), \\ f_{-1}(x_k^{(0)}) + f_0(x_k^{(0)}) &= \mathbf{I}_{V0}f(x_k^{(0)}) + (\mathbf{f}_k^{(0)} - (\mathbf{I}_{V0}f)_k^{(0)}) = f(x_k^{(0)}). \end{aligned} \tag{3.14}$$

Equation (3.14) implies that function $f_{-1}(x) + f_0(x)$ actually interpolates $f(x)$ on both interpolation points $\{x_k^{(-1)}\}_{k=1}^{L-1}$ for V_0 and the interpolation points $\{x_k^{(0)}\}_{k=-1}^{L-2}$ for W_0.

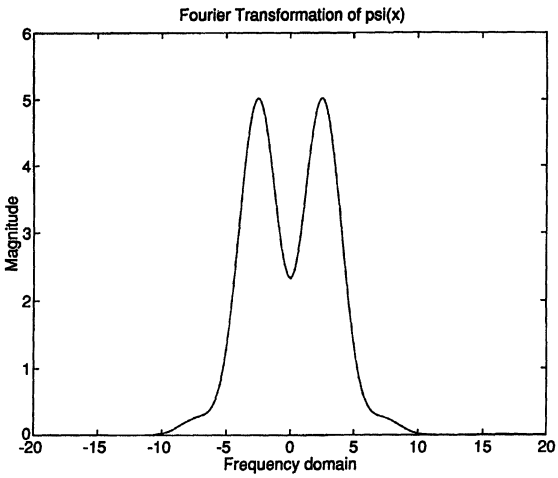

FIG. 3. *Fourier transformations of* $\psi(x)$.

Step 3. Generally, we define, for $1 \le j \le J-1$,

$$f_j(x) = \mathbf{I}_{W_j}(\mathbf{f}^{(j)} - (\mathcal{P}_{j-1}f)^{(j)}) \tag{3.15}$$

$$= \sum_{k=-1}^{n_j-2} \hat{f}_{j,k}\psi_{j,k}(x), \tag{3.16}$$

where $(\mathcal{P}_{j-1}f)_k^{(j)} = \mathcal{P}_{j-1}f(x_k^{(j)})$, $-1 \le k \le n_j - 2$.

Again, as in Step 2, we can verify that function $f_{-1}(x)+f_0(x)+\cdots+f_{j-1}(x)$ interpolates function $f(x)$ on all interpolation points $\{x_k^{(-1)}\}_{k=1}^{L-1}, \ldots, \{x_k^{(j-1)}\}_{k=-1}^{n_{j-1}-2}$. Specifically, for $j = J$ we have $\mathcal{P}_J f(x) = f_{-1}(x)+f_0(x)+\cdots+f_{J-1}(x)$, which satisfies the required interpolation condition (3.11).

Number of operations. For $j = -1$, the number of operations to invert (3.9) by using the Thomas algorithm to obtain $\{\hat{f}_k^{(-1)}\}$ is $8(L-1)$(flops). For $0 \le j \le J-1$, the cost of computing the coefficients $\hat{f}_k^{(j)}$ in $f_j(x) = \mathbf{I}_{W_j}(f^{(j)} - (\mathcal{P}_{j-1}f)^{(j)}) = \sum_{-1\le k\le n_j-2} \hat{f}_{j,k}\psi_{j,k}(x)$ has three parts: (1) evaluating $(\mathcal{P}_{j-1}f)^{(j)} = \{\mathcal{P}_{j-1}f(x_k^{(j)})\} - 5jn_j$(flops); (2) calculating the difference $f^{(j)} - (\mathcal{P}_{j-1}f)^{(j)} - n_j$(flops); (3) inverting the matrix $\mathbf{M}_j$ in (3.9) - $8n_j$(flops). So the total cost of finding $\hat{\mathbf{f}} = 8(L-1) + \sum_{j=0}^{(J-1)}(5j+9)n_j \le 6N \log N$ where, again, $N = 2^J L - 1$.

3.5. Wavelet expansion coefficients $\{\hat{f}_{j,k}\}$. First we consider the Fourier transformation of the wavelet function $\psi(x)$,

$$\hat{\psi}(\omega) = \frac{7}{3}(2-\cos\omega)\left(\frac{\sin\frac{\omega}{4}}{\frac{\omega}{4}}\right)^4 e^{-\frac{3\omega}{2}i}. \tag{3.17}$$

We find that $\hat{\psi}(0) = \frac{7}{3}$, which means that $\psi(x)$ has no vanishing moment of the first order (see Figure 3). Since the wavelet decomposition we consider here is in the space $H_0^2(I)$, the decaying properties for the wavelet coefficients $\{\hat{f}_{j,k}\}$ ought to be related to the vanishing moments of the second derivative of $\psi(x)$ (see Figure 4), not to those of $\psi(x)$. To clarify the meaning of the wavelet coefficients $\{\hat{f}_{j,k}\}$ in the finite wavelet decomposition of function

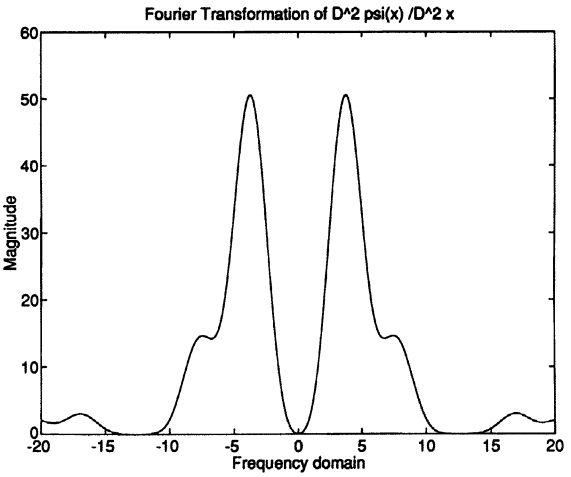

FIG. 4. *Fourier transformations of* $\psi''(x)$.

$f(x)$ in $H_0^2(I)$, let us consider the dual basis $\{\psi_{j,k}^*(x)\}$ for $\{\psi_{j,k}(x)\}$ in W_j, i.e.,

$$\int_I (\psi_{j,k}^*)''(x)(\psi_{j,l})''(x)\,dx = \delta_{lk}. \tag{3.18}$$

Since W_j, $j = 0, \ldots, J-1$, and V_0 are mutually orthogonal, we have

$$\hat{f}_{j,k} = \int_I f''(x)(\psi_{j,k}^*)''(x)dx. \tag{3.19}$$

We need to express $\psi_{j,k}^*(x)$ in terms of $\{\psi_{j,k}(x)\}_{k=-1}^{n_j-2}$, namely,

$$\psi_{j,k}^*(x) = \sum_{l=-1}^{n_j-2} \beta_{kl}^{(j)*}\psi_{j,l}(x), \tag{3.20}$$

where the coefficients $\beta_{kl}^{(j)*}$ are determined as follows.

Let $\mathbf{G_j}$ denote the matrix

$$\mathbf{G_j} = (\beta_{kl}^{(j)})_{n_j \times n_j}, \tag{3.21}$$

where $\beta_{kl}^{(j)} = \int_I \psi_{j,k}''(x)\psi_{j,l}''(x)\,dx$, $-1 \le k, l \le n_j - 2$. Then, from (3.18) we have

$$(\beta_{kl}^{(j)*})_{n_j \times n_j} = \mathbf{G_j}^{-1}. \tag{3.22}$$

To estimate the entries of matrix $(\beta_{kl}^{(j)*})_{n_j \times n_j}$, we recall that

$$\begin{aligned}\beta_{kl}^{(j)} &= \int_I \psi_{j,k}''(x)\psi_{j,l}''(x)\,dx \\ &= 2^{3j}\int_{2^j I} \psi_{0,k}''(x)\psi_{0,l}''(x)\,dx \\ &= 2^{3j}\int_{2^j I} \psi_{0,k}^{(4)}(x)\psi_{0,l}(x)\,dx\end{aligned}$$

and that $\psi_{0l}(n) = 0, n \in Z$, $\psi(\frac{1}{2}) = -\frac{1}{14}$, $\psi(\frac{3}{2}) = 1$, $\psi(\frac{5}{2}) = -\frac{1}{14}$, $\psi_b(\frac{1}{2}) = 1$, $\psi_b(\frac{3}{2}) = -\frac{1}{13}$, $\psi^{(4)}(\frac{1}{2}) = 2^8 \times \frac{3}{14}\delta(x - \frac{1}{2})$, $\psi^{(4)}(\frac{3}{2}) = 2^8 \times \frac{12}{14}\delta(x - \frac{3}{2})$, $\psi^{(4)}(\frac{5}{2}) = 2^8 \times \frac{3}{14}\delta(x - \frac{5}{2})$, $\psi_b^{(4)}(\frac{1}{2}) = 2^8 \times \frac{15}{13}\delta(x - \frac{1}{2})$, and $\psi_b^{(4)}(\frac{3}{2}) = 2^8 \times \frac{3}{13}\delta(x - \frac{3}{2})$. Thus we have the following:

$$\mathbf{G_j} = \frac{6}{7} \times 2^{3(j+2)} \begin{pmatrix} \frac{896}{169} & \frac{9}{13} & -\frac{1}{13} & 0 & & & & & & \\ \frac{9}{13} & \frac{54}{14} & \frac{10}{14} & -\frac{1}{14} & & & & & & \\ -\frac{1}{13} & \frac{10}{14} & \frac{54}{14} & \frac{10}{14} & \ddots & & & & & \\ 0 & -\frac{1}{14} & \frac{10}{14} & \frac{54}{14} & \ddots & \ddots & & & & \\ & & \ddots & \ddots & \ddots & \ddots & \ddots & & & \\ & & & \ddots & \ddots & \frac{54}{14} & \frac{10}{14} & -\frac{1}{14} & 0 & \\ & & & & \ddots & \frac{10}{14} & \frac{54}{14} & \frac{10}{14} & -\frac{1}{13} & \\ & & & & & -\frac{1}{14} & \frac{10}{14} & \frac{54}{14} & \frac{9}{13} & \\ & & & & & 0 & -\frac{1}{13} & \frac{9}{13} & \frac{896}{169} & \end{pmatrix}$$

$$= \frac{6}{7} \times 2^{3(j+2)} \Gamma_j.$$

$\Gamma_j = (\gamma_{kl})_{n_j \times n_j}$ is actually a Hermite matrix satisfying

$$\gamma_{kk} - \sum_{l=-1, l\neq k}^{n_j-2} |\gamma_{kl}| \geq C > 0, \qquad -1 \leq k \leq n_j - 2,$$

where C is a constant independent of j. Hence there exist two positive constants C_1 and C_2, which are independent of j, such that

$$C_1 I_{nj} \leq \Gamma_j \leq C_2 I_{nj},$$

where I_{nj} is the $n_j \times n_j$ identity matrix. Now denote

$$\Gamma_j^{-1} = (\gamma_{kl}^*)_{n_j \times n_j}.$$

By using Lemmas 8 and 9 in [23], we assert that there are two positive constants K and γ such that

$$|\gamma_{kl}^*| \leq K \exp(-\gamma |k - l|).$$

Since

$$(\beta_{kl}^{(j)*})_{n_j \times n_j} = \frac{7}{6} \times 2^{-3(j+2)} \Gamma_j^{-1},$$

we have

$$|\beta_{kl}^{(j)*}| \leq K_1 2^{-3j} \exp(-\gamma |k - l|). \tag{3.23}$$

To estimate the coefficients $\hat{f}_{jk}$ in (3.19), we use the following result from Meyer's book [8].

LEMMA 4. *Let $g(x)$ be compactly supported, be n times continuously differentiable, and have $n + 1$ vanishing moments:*

$$\int_{-\infty}^{\infty} x^p g(x) dx = 0 \quad \textit{for } 0 \leq p \leq n.$$

Let $\alpha, 0 < \alpha < n$, be a real number that is not an integer and $f(x) \in L^2$. Then $f(x)$ is uniformly Lipschitz of order α over a finite interval $[a, b]$ if and only if for any $k \in Z$ and $j \in Z$ such that $2^{-j}k \in (a, b)$,

$$\left| \int f(x) g(2^j x - k)\, dx \right| = O(2^{-(\alpha+1)j}) \quad \text{as } j \to \infty. \tag{3.24}$$

Applying this lemma, we can prove the following result.

LEMMA 5. *Let $0 < \alpha < 1$ and $f \in H_0^2(I)$. If the second derivative of the function f is Hölder continuous with exponent α, at $x_0 \in I$, i.e.,*

$$|f''(x) - f''(x_0)| \le C|x - x_0|^\alpha, \qquad x \in (x_0 - \delta, x_0 + \delta) \subset I$$

for some $\delta > 0$, then for any $k \in Z$, $j \in Z^+$ such that $2^{-j}k \in (x_0 - \delta/2, x_0 + \delta/2)$,

$$|\hat{f}_{j,k}| = O(2^{-(\alpha+2)j}) \quad \text{as } j \to \infty. \tag{3.25}$$

Proof. Since ψ and ψ_b, defined by (2.21) and (2.22), are two times continuously differentiable and their second derivatives have two vanishing moments, by Lemma 4,

$$\begin{aligned}
|\hat{f}_{j,k}| = |\langle f, \psi^*_{j,k}\rangle| &\le \sum_{2^{-j}l \in (x_0-\delta, x_0+\delta)} |\beta^{(j)*}_{kl}|\, |\langle f, \psi_{j,l}\rangle| \\
&\quad + \sum_{2^{-j}l \bar{\in} (x_0-\delta, x_0+\delta)} |\beta^{(j)*}_{kl}|\, |\langle f, \psi_{jl}\rangle| \\
&\le \left(\sum_{2^{-j}l \in (x_0-\delta, x_0+\delta)} + \sum_{2^{-j}l \bar{\in} (x_0-\delta, x_0+\delta)} \right) K_1 2^{-3j} \exp(-\gamma|k-l|) 2^{2j} \left| \int_R f''(x) \psi''(2^j x - l)\, dx \right| \\
&\le \left[\sum_{2^{-j}l \in (x_0-\delta, x_0+\delta)} K_1 \exp(-\gamma|k-l|) \right] O(2^{-(\alpha+2)j}) + K_2 \exp\left(-\frac{1}{2}\delta\gamma 2^j\right) \sum_{s=1}^{\infty} \exp(-\gamma s) \\
&= O(2^{-(\alpha+2)j}). \qquad \square
\end{aligned}$$

Lemma 5 implies that the wavelet coefficients $\hat{f}_{jk}$, $j \ge 0$, reflect the singularity of the function to be approximated. In practice, when we solve PDEs using collocation methods, we often use the values of the functions, not their derivatives. Therefore, to use the wavelet coefficients to adjust the choice of wavelet basis functions, we have to establish a relation between the magnitudes of the wavelet coefficients $\hat{f}_{j,k}$, $j \ge 0$, and $f(x)$. Let us first state the following result on the inverse of the tridiagonal matrix from [24].

LEMMA 6. *Let A be an $n \times n$ tridiagonal matrix with elements $a_2, a_3, \ldots, a_n$ on the subdiagonal, $b_1, b_2, \ldots, b_n$ on the diagonal, and $c_2, c_3, \ldots, c_n$ on the superdiagonal, where $a_i, c_i \neq 0$. Define the two sequences $\{u_m\}$, $\{v_m\}$ as follows:*

$$u_0 = 0, \quad u_1 = 1, \quad u_m = -\frac{1}{c_m}(a_{m-1}u_{m-2} + b_{m-1}u_{m-1}), \qquad m \ge 2, \tag{3.26}$$

$$v_{n+1} = 0, \quad v_n = 1, \quad v_m = -\frac{1}{a_{m+1}}(b_{m+1}v_{m+1} + c_{m+2}v_{m+2}), \qquad m \le n-1, \tag{3.27}$$

where a_1 and c_{n+1} are arbitrary nonzero constants. Then $A^{-1} = (\alpha_{i,j})$ is given by

$$\alpha_{ij} = \begin{cases} -\frac{u_i v_j}{a_1 v_0} \prod_{k=2}^{j} \frac{c_k}{a_k}, & i \le j, \\ -\frac{u_j v_i}{a_1 v_0} \prod_{k=2}^{j} \frac{c_k}{a_k}, & i > j. \end{cases} \tag{3.28}$$

COROLLARY. *Let M_j be the interpolation matrix in* (3.9). *Then we have the following estimates on $M_J^{-1} = (\alpha_{i,j})$:*

$$|\alpha_{i,j}| \le \frac{K}{\alpha^{|j-i|}}, \tag{3.29}$$

where $K = 1.1726$ and $\alpha = 7 + \sqrt{192} \doteq 13.928$.

We delay the proof of (3.29) to the Appendix.

THEOREM 3. *Let $f(x) \in H_0^2(0, L)$, $M = \max_I |f(x)|$, and $\mathbf{I}_{W_j} f(x)$ be its interpolation in W_j defined in* (3.8). *If for $\epsilon > 0$, $-1 \le k_1 < k_2 \le n_j - 2$,*

$$|f(x_k^{(j)})| \le \epsilon \quad \text{for } k_1 \le k \le k_2,$$

defining

$$\tilde{\mathbf{I}}_{w_j} f(x) = \sum_{-1 \le k \le n_j - 2, k \in [k_1 + l, k_2 - l]} \hat{f}_{j,k} \psi_{j,k}(x), \tag{3.30}$$

where $l = l(\epsilon) = \min(\frac{n_j}{2}, -\frac{\log \epsilon}{\log \alpha})$, then we have

$$|\tilde{\mathbf{I}}_{w_j} f(x) - \mathbf{I}_{W_j} f(x)| \le C(M)\epsilon, \tag{3.31}$$

where $C(M) = \frac{6K}{\alpha - 1}(\alpha + M)$, $K = 1.1726$, and $\alpha = 7 + \sqrt{192} \doteq 13.928$.

Proof. From (3.9), we have

$$\hat{\mathbf{f}}^{(j)} = \mathbf{M}_j^{-1} \mathbf{f}^{(j)},$$

where $\hat{\mathbf{f}}^{(j)} = (\hat{f}_{j,-1}, \dots, \hat{f}_{j,n_j-2})^\top$, $\mathbf{f}^{(j)} = (f(x_{-1}^{(j)}), \dots, f(x_{n_j-2}^{(j)}))^\top$. Thus

$$\hat{f}_{j,k} = \sum_{i=1}^{n_j} \alpha_{k,i} f(x_{i-2}^{(j)}), \qquad -1 \le k \le n_j - 2.$$

So we have

$$|\hat{f}_{j,k}| \le K \sum_{i=1}^{n_j} \frac{1}{\alpha^{|k-i|}} |f(x_{i-2}^{(j)})|. \tag{3.32}$$

For any given $\epsilon > 0$, we take $\ell = \min(\frac{n_j}{2}, -\log_{\frac{\epsilon}{\log}} \alpha)$. For $k \in [k_1 + \ell, k_2 - \ell]$, using (3.32) we have

$$\begin{aligned}
|\hat{f}_{j,k}| &\le K \left[\sum_{|k-i| \le \ell} \frac{1}{\alpha^{|k-i|}} |f(x_{i-2}^{(j)})| + \sum_{|k-i| > \ell} \frac{1}{\alpha^{|k-i|}} |f(x_{i-2}^{(j)})| \right] \\
&\le K\epsilon \sum_{|k-i| \le \ell} \frac{1}{\alpha^{|k-i|}} + MK \sum_{|k-i| > \ell} \frac{1}{\alpha^{|k-i|}} \\
&\le 2K\epsilon \left[1 + \left(\frac{1}{\alpha}\right) + \cdots + \left(\frac{1}{\alpha}\right)^{\ell} \right] + 2MK \left[\left(\frac{1}{\alpha}\right)^{\ell+1} + \cdots + \left(\frac{1}{\alpha}\right)^{n_j - \ell} \right] \\
&= 2K\epsilon \frac{1 - (\frac{1}{\alpha})^{\ell+1}}{1 - (\frac{1}{\alpha})} + 2MK \left(\frac{1}{\alpha}\right)^{\ell+1} \frac{1 - (\frac{1}{\alpha})^{n_j - 2\ell}}{1 - (\frac{1}{\alpha})} \\
&\le 2K\epsilon \frac{\alpha}{\alpha - 1} + 2MK\epsilon \frac{1}{\alpha - 1} \\
&= C'\epsilon,
\end{aligned}$$

where $C' = \frac{2K}{\alpha - 1}(\alpha + M)$.

Finally, we have

$$|\tilde{\mathbf{I}}_{w_j} f(x) - \mathbf{I}_{W_j} f(x)| = \left| \sum_{k\in[k_1+\ell,k_2-\ell]} \hat{f}_{j,k}\psi_{j,k}(x) \right|$$
$$\leq \sum_{k\in[k_1+\ell,k_2-\ell]} |\hat{f}_{j,k}||\psi_{j,k}(x)| \leq C'\epsilon \sum_{k\in[k_1+\ell,k_2-\ell]} |\psi_{j,k}(x)|.$$

Note that in the last summation, only three terms will be nonzero for any fixed x, so we have

$$|\tilde{\mathbf{I}}_{w_j} f(x) - \mathbf{I}_{W_j} f(x)| \leq 3C'\epsilon = C\epsilon,$$

where $C = \frac{6K}{\alpha-1}(\alpha + M)$. This concludes the proof of Theorem 3. □

Remark. As a consequence of Theorem 3, the coefficients $\hat{f}_{j,k}$ of the wavelet interpolation operator $\mathbf{I}_{W_j} f(x)$ can be ignored if the magnitudes of function $f(x)$ at points $x_k^{(j)} \in [x_{k_1+\ell}^{(j)}, x_{k_2-\ell}^{(j)}]$ are less than some given error tolerance ϵ. This procedure will only result in an error of $O(\epsilon)$. For $\epsilon = 10^{-10}$, $\ell = 9$ and for $\epsilon = 10^{-8}$, $\ell = 7$. In the wavelet interpolation expansion (3.10), $\mathbf{I}_{W_j}$ is used to interpolate the difference between a lower-level interpolation $\mathcal{P}_{j-1}f(x)$ and $f(x)$, i.e., $\mathcal{P}_{j-1}f(x) - f(x)$. Thus, the function $\mathcal{P}_{j-1}f(x) - f(x)$ will be the function occurring in Theorem 3 (recall that in Theorem 3 that function is still denoted by $f(x)$ for the sake of simpler notation). Hence, the coefficients $\hat{f}_{j,k}$ in the wavelet expansion will be less than the error tolerance ϵ in a larger region of the solution domain as j becomes larger. Then many terms of $\psi_{j,k}(x)$ can be discarded in the wavelet expansion of $f(x)$. This fact will be used later to achieve adaptivity for the solution of PDEs. The idea of decomposing numerical approximations into different scales has been previously used successfully in the shock-wave computations with uniform high-order spectral methods, where essential nonoscillatory (ENO) finite difference methods and spectral methods are combined to resolve the shocks and the high-frequency components in the solution, respectively [25].

We conclude this section with the following result which shows how to use wavelet coefficients to estimate the data interpolated by $\mathbf{I}_{W_j}$.

THEOREM 4. *Let* $\mathbf{I}_{W_j} f(x)$ *and* $f(x)$ *be defined as in Theorem* 3. *For* $\epsilon > 0$, $-1 \leq k_1 < k_2 \leq n_j - 2$, *if*

$$|\hat{f}_{j,k}| \leq \epsilon \quad \text{for } k_1 \leq k \leq k_2,$$

then

$$|f(x_k^{(j)})| \leq 3\epsilon \quad \text{for } k_1 + 3 \leq k \leq k_2 - 3. \tag{3.33}$$

Proof. The proof follows from the definition of $\mathbf{I}_{W_j} f(x)$. □

4. Derivative matrices. The operation of differentiation of functions, given by its wavelet expansion of (3.10), can be represented by a finite dimension matrix $\mathcal{D}$. Such a matrix has been investigated in [26] for wavelet approximation of periodic functions based on Daubechies' compactly supported wavelets. The properties of matrix $\mathcal{D}$, especially of its eigenvalues, greatly affect the efficiency and stability of the numerical methods for the solution of time-dependent PDEs.

Because of the multiresolution structure of spaces V_j, $V_j \subset V_{j+1}$ and $V_0 \oplus W_0 \oplus \cdots \oplus W_J = V_{J+1}$. We can assume that $J + 1 = 0$ and the wavelet interpolation $u_0(x)$ for function $u(x)$ can be written as a linear combination of $\mathbf{I}_{b,0}u(x)$ and basis in V_0, namely,

$$u_0(x) = \mathbf{I}_{b,0}u(x) + \hat{u}_{-1}\phi_{b,0}(x) + \sum_{k=0}^{L-4} \hat{u}_k\phi_{0,k}(x) + \hat{u}_{L-3}\phi_{b,0}(L-x). \tag{4.1}$$

Here we only consider the case where $\mathbf{I}_{b,0}u(x)$ is defined in (2.35) with end-derivative condition (2.36)-(2.39). The case of not-a-knot conditions can be treated similarly.

4.1. Second derivative matrix. Consider the second derivative matrix which approximates the second differential operator

$$\mathcal{L}u = u_{xx} \tag{4.2}$$

with the boundary conditions

$$u(0) = u(L) = 0. \tag{4.3}$$

As $u_0(x)$ is a cubic spline interpolant of function $u(x)$ based on the knots $x_i = i, i = 0, \ldots, L$ with the end derivatives given by (2.39), from the first and second derivative continuity condition of $u_0(x)$ we have

$$u_i' = \frac{h_i}{6}u_{i-1}'' + \frac{h_i}{3}u_i'' + \frac{u_i - u_{i-1}}{h_i}, \qquad 1 \le i \le L, \tag{4.4}$$

$$u_{i-1}' = -\frac{h_i}{3}u_{i-1}'' - \frac{h_i}{6}u_i'' + \frac{u_i - u_{i-1}}{h_i}, \qquad 1 \le i \le L, \tag{4.5}$$

and

$$\frac{h_i}{hi + h_{i+1}}u_i'' + 2u_i'' + \frac{h_{i+1}}{h_i + h_{i+1}}u_{i+1}'' = \frac{6}{h_i + h_{i+1}}\left[\frac{u_{i+1} - u_i}{h_{i+1}} - \frac{u_i - u_{i-1}}{h_i}\right], \tag{4.6}$$

where $1 \le i \le L-1$, $u_i' = u'(x_i)$, $u_i'' = u''(x_i)$, and $h_i = x_i - x_{i-1} = 1$.

Equations for the second derivatives at x_i, $1 \le i \le L-1$, are provided by (4.6) while the equations for the second derivatives at two end points can be obtained from (4.5) ($i = 1$) and (4.4) ($i = L$):

$$\frac{h_1}{3}u_0'' + \frac{h_1}{6}u_1'' = \frac{u_1 - u_0}{h_1} - \dot{u}_0, \tag{4.7}$$

$$\frac{h_L}{6}u_{L-1}'' + \frac{h_L}{3}u_L'' = \dot{u}_L - \frac{u_L - u_{L-1}}{h_L}, \tag{4.8}$$

where $\dot{u}_0, \dot{u}_L$ are the approximations of the first derivative of $u(x)$ at x_0, x_L in (2.39), respectively.

Using the notation

$$\mathbf{u} = (u(0), u(1), \ldots, u(L))^\top \in \mathbf{R}^{L+1},$$
$$\mathbf{u}'' = (u''(0), u''(1), \ldots, u''(L))^\top \in \mathbf{R}^{L+1},$$

from (4.6), (4.7), and (4.8) we have the following:

$$\mathbf{T}_1\mathbf{u}'' = \mathbf{T}_2\mathbf{u} + \vec{\gamma}, \tag{4.9}$$

where

$$\mathbf{T}_1 = \begin{pmatrix} \frac{h_1}{3} & \frac{h_1}{6} & 0 & & & & & \\ \frac{h_1}{h_1+h_2} & 2 & \frac{h_2}{h_1+h_2} & & & & & \\ & \ddots & \ddots & \ddots & & & & \\ & & \frac{h_i}{h_i+h_{i+1}} & 2 & \frac{h_{i+1}}{h_i+h_{i+1}} & & & \\ & & & \ddots & \ddots & \ddots & & \\ & & & & \frac{h_{L-1}}{h_{L-1}+h_L} & 2 & \frac{h_L}{h_{L-1}+h_L} & \\ & & & & & \frac{h_L}{6} & \frac{h_L}{3} \end{pmatrix},$$

$$\mathbf{T}_2 = \begin{pmatrix} -\frac{1}{h_1} & \frac{1}{h_1} & & & & \\ \frac{6}{h_1(h_1+h_2)} & -\frac{6}{h_1+h_2}\left(\frac{1}{h_1}+\frac{1}{h_2}\right) & \frac{6}{h_2(h_1+h_2)} & & & \\ & \ddots & \ddots & \ddots & & \\ & & \frac{6}{h_{L-1}(h_{L-1}+h_L)} & -\frac{6}{h_{L-1}+h_L}\left(\frac{1}{h_{L-1}}+\frac{1}{h_L}\right) & \frac{6}{h_L(h_{L-1}+h_L)} & \\ & & & \frac{1}{h_L} & -\frac{1}{h_L} \end{pmatrix},$$

$$\vec{\gamma} = \begin{pmatrix} \dot{u}_0 \\ 0 \\ \vdots \\ 0 \\ \dot{u}_L \end{pmatrix} = \begin{pmatrix} \vec{\alpha} \\ 0 \\ \vdots \\ 0 \\ \vec{\beta} \end{pmatrix} \mathbf{u} = \Gamma \mathbf{u},$$

and

$$\vec{\alpha} = \frac{1}{h}(c_0, \ldots, c_p, 0, \ldots, 0)^\top \in R^{L+1}, \qquad \vec{\beta} = \frac{1}{h}(0, \ldots, 0, c_p, \ldots, c_0)^\top \in R^{L+1},$$

with $c_0', \ldots, c_p'$ defined in (2.39).

As a result of the uniqueness of the spline $u_0(x)$, $\mathbf{T}_1$ is invertible, so we have

$$\mathbf{u}'' = \mathbf{T}_1^{-1}(\mathbf{T}_2 + \Gamma)\mathbf{u} = \mathcal{D}_2\mathbf{u}. \tag{4.10}$$

By eliminating the first and last rows and columns, we then obtain the second derivative matrix for the differential operator (4.2).

4.2. First derivative matrix. Here we consider the first derivative matrix which approximates the first differential operator

$$\mathcal{L}u = u_x \tag{4.11}$$

with the boundary condition

$$u(L) = 0. \tag{4.12}$$

Using the notation

$$\mathbf{u}' = (u'(0), u'(1), \ldots, u'(L))^\top \in \mathbf{R}^{L+1},$$

and using (4.4) and (4.5), we have

$$\mathbf{u}' = \mathbf{H}_1\mathbf{u}'' + \mathbf{H}_2\mathbf{u}, \tag{4.13}$$

where

$$\mathbf{H}_1 = \begin{pmatrix} -\frac{h_1}{3} & -\frac{h_1}{6} & & & & & & \\ \frac{h_1}{6} & \frac{h_1}{3} & 0 & & & & & \\ & \frac{h_2}{6} & \frac{h_2}{3} & 0 & & & & \\ & & \ddots & \ddots & \ddots & & & \\ & & & \frac{h_i}{6} & \frac{h_i}{3} & 0 & & \\ & & & & \ddots & \ddots & \ddots & \\ & & & & & \frac{h_{L-1}}{6} & \frac{h_{L-1}}{3} & 0 \\ & & & & & & \frac{h_L}{6} & \frac{h_L}{3} \end{pmatrix}$$

and

$$\mathbf{H}_2 = \begin{pmatrix} -\frac{1}{h_1} & \frac{1}{h_1} & & & & & & & \\ -\frac{1}{h_1} & \frac{1}{h_1} & 0 & & & & & & \\ & -\frac{1}{h_2} & \frac{1}{h_2} & 0 & & & & & \\ & & \ddots & \ddots & \ddots & & & & \\ & & & -\frac{1}{h_i} & \frac{1}{h_i} & 0 & & & \\ & & & & \ddots & \ddots & \ddots & & \\ & & & & & -\frac{1}{h_{L-1}} & \frac{1}{h_{L-1}} & 0 & \\ & & & & & & -\frac{1}{h_L} & \frac{1}{h_L} & \end{pmatrix}.$$

Finally, by using (4.10) we obtain

$$\mathbf{u}' = (\mathbf{H}_1\mathcal{D}_2 + \mathbf{H}_2)\mathbf{u} = \mathcal{D}_1\mathbf{u}, \tag{4.14}$$

and, after eliminating the last row and column of $\mathcal{D}_1$, we also have the first derivative matrix for the differential operator (4.11).

In Figure 15, we plot the eigenvalues of $\mathcal{D}_1$ for $L = 8$, $J = 0, 1, 2, 3$, which correspond to $N = 8, 16, 32, 64$. The eigenvalues come in conjugate pairs with two pure real eigenvalues. The real parts of all the eigenvalues are negative. The largest eigenvalue increases in the order of $O(N)$ in magnitude. In Figure 16, we plot the eigenvalues of $\mathcal{D}_2$ for $L = 8$, $J = 0, 1, 2, 3$, which correspond to $N = 8, 16, 32, 64$. They are all real and positive and the largest one increases in the order of $O(N^2)$.

5. Adaptive wavelet collocation methods for PDEs. In this section we consider a collocation method based on the DWT described in §3 for time-dependent PDEs. Let $u = u(x, t)$ be the solution of the following initial boundary value problem:

$$\begin{cases} u_t + f_x(u) = u_{xx} + g(u), & x \in [0, L], t \geq 0, \\ u(0, t) = g_0(t), \\ u(L, t) = g_1(t), \\ u(x, 0) = f(x). \end{cases} \tag{5.1}$$

Here only Dirichlet boundary conditions are considered, however, the methods can also be modified to treat Von Neumann-type or Robin-type boundary conditions.

We use the idea of the method of lines where only the spatial derivative is discretized by the wavelet approximation. The numerical solution $u_J(x, t)$ will be represented by a unique decomposition in $V_0 \oplus W_0 \oplus \cdots \oplus W_{J-1}$, $J - 1 \geq 0$, namely,

$$\begin{aligned} u_J(x, t) &= \mathbf{I}_{b,J}u(x, t) + \hat{u}_{-1,-1}(t)\phi_b(x) + \sum_{k=0}^{L-4} \hat{u}_{-1,k}(t)\phi_k(x) + \hat{u}_{-1,L-3}(t)\phi_b(L - x) \\ &\quad + \sum_{j=0}^{J-1} \left[\sum_{k=-1}^{n_j-2} \hat{u}_{j,k}(t)\psi_{j,k}(x) \right] \\ &= u_{-1}(x) + \sum_{j=0}^{J-1} u_j(x), \end{aligned} \tag{5.2}$$

where $\mathbf{I}_{b,J}u(x, t)$ given in (2.35) consists of the nonhomogeneity of $u(x, t)$ on both boundaries, and the coefficients $\hat{u}_{j,k}(t)$ are all functions of t. Using the DWT, we can also identify the numerical solution $u_J(x, t)$ by its point values on all collocation (previously named interpolation)

points, i.e., $\{x_k^{(j)}\}$ in (3.1) and (3.6). We put all these values in vector $\mathbf{u} = \mathbf{u}(t)$, i.e.,

$$\mathbf{u} = \mathbf{u}(t) = (\mathbf{u}^{(-1)}, \mathbf{u}^{(0)}, \ldots, \mathbf{u}^{(J-1)})^\top,$$

where $\mathbf{u}^{(j)} = \{u(x_k^{(j)}, t)\}$, $1 \le k \le L-1$, for $j = -1$; $-1 \le k \le n_j - 2$, for $j \ge 0$.

To solve for the unknown solution vector $\mathbf{u}(t)$, we collocate the PDE (5.1) on all collocation points and obtain the following semidiscretized wavelet collocation method.

5.1. Semidiscretized wavelet collocation method.

$$\text{(5.3)} \quad \begin{cases} u_{J_t} + f_x(u_J) = R(u_{J_{xx}}) + g(u_J)|_{x=x_k^{(j)}}, & -1 \le j \le J-1, \\ u_J(0,t) = g_0(t), \\ u_J(L,t) = g_1(t), \\ u_J(x_k^{(j)}, 0) = f(x_k^{(j)}), \end{cases}$$

where $1 \le k \le L-1$, for $j = -1$; $-1 \le k \le n_j - 2$, for $j \ge 0$. The average operator R on the second derivative is used to take advantage of the superconvergence of the cubic spline at the knot points (see (2.17)). However, R should only be used at a local uniform mesh [19].

Equation (5.3) involves a total of $(2^J - 1)L + 2$ unknowns in $\mathbf{u}$; two of them will be determined by the boundary conditions and the rest are the solutions of the ordinary differential equation (ODE) system subject to their initial conditions. To implement the time marching scheme for the ODE's system (e.g., Runge–Kutta-type time integrator), we have to compute the derivative term in (5.3) $f_x(u_J(x_k^{(j)}))$ and $u_{J_{xx}}(x_k^{(j)})$ in an efficient way. Let us only discuss the first derivative which involves the computation of the nonlinear function $f(u_J(x,t))$. For this purpose we first find a similar wavelet decomposition as (5.2) for $f(u_J)$. For a general nonlinear function $f(u)$, this can be done in a straightforward manner by using the DWT in §3.

5.2. Computation of $f_x(x_k^{(j)}) = f_x(u_J(x_k^{(j)}))$.

Step 1. Given $\mathbf{u} = (\mathbf{u}^{(-1)}, \mathbf{u}^{(0)}, \ldots, \mathbf{u}^{(J-1)})^\top$, compute $\mathbf{f}^{(j)} = \{f(u_k^{(j)})\}$, $j \ge -1$, and define

$$\mathbf{f} = (\mathbf{f}^{(-1)}, \mathbf{f}^{(0)}, \ldots, \mathbf{f}^{(J-1)})^\top.$$

Step 2. Compute the wavelet interpolation expansion using DWT for $\mathbf{f}$:

$$\text{(5.4)} \quad \begin{aligned} f_J(x,t) = \mathbf{I}_{b,J} f + \hat{f}_{-1,-1}(t)\phi_b(x) + \sum_{k=0}^{L-4} \hat{f}_{-1,k}(t)\phi_k(x) + \hat{f}_{-1,L-3}(t)\phi_b(L-x) \\ + \sum_{j=0}^{J-1} \left[\sum_{k=-1}^{n_j-2} \hat{f}_{j,k}(t)\psi_{j,k}(x) \right]. \end{aligned}$$

Step 3. Differentiate (5.4) and evaluate it at all collocation points $\{x_k^{(j)}\}$, $j \ge -1$:

$$\begin{aligned} f_x(u_J)|_{x=x_k^{(j)}} = (\mathbf{I}_{b,J} f)'(x_k^{(j)}) + \hat{f}_{-1,-1}(t)\phi_b'(x_k^{(j)}) \\ + \sum_{k=0}^{L-4} \hat{f}_{-1,k}(t)\phi_k'(x_k^{(j)}) - \hat{f}_{-1,L-3}(t)\phi_b'(L - x_k^{(j)}) \\ + \sum_{i=0}^{J} \left[\sum_{l=-1}^{n_i-2} \hat{f}_{i,l}(t)\psi_{i,l}'(x_k^{(j)}) \right]. \end{aligned}$$

5.2.1. Cost of computing the derivatives. For each single collocation point, it takes $7 + 5(J+1) = 5J + 12$(flops) to compute $f'_J(x_k^{(J)})$. Therefore, the total cost of computing all derivatives is $(5J+12)N \le 5N \log N$. Again, $\psi'(x)$ and $\phi'(x)$ at the dyadic points $\frac{k}{2^j}$, $0 \le k \le 2^j L$, can be precomputed for future use.

Assuming that the Euler forward difference scheme is used to discretize the time derivative in (5.3), we obtain a fully discretized wavelet collocation method.

5.3. Fully discretized wavelet collocation method.

$$\text{(5.5)} \quad \begin{cases} u_J{}^{n+1} = u_J{}^n + \Delta t[-f_x(u_J^n) + R(u^n_{J_{xx}}) + g(u_J^n)]|_{x=x_k^{(j)}}, & -1 \le j \le J-1, \\ u_J^n(0) = g_0(t^n), \\ u_J^n(L) = g_1(t^n), \\ u_J^0(x_k^{(j)}) = f(x_k^{(j)}), \end{cases}$$

where $1 \le k \le L-1$, for $j = -1$; $-1 \le k \le n_j - 2$, for $j \ge 0$; $t^n = n\Delta t$ is the time station; and Δt is the time step.

5.4. Adaptive choice of collocation points. In equations (5.2) and (5.4), $u_J(x)$ and $f(u_J(x))$ are expressed using the full set of collocation points $\{x_k^{(j)}\}$. As discussed in the remark after Theorem 3, most of the wavelet expansion coefficients $\hat{u}_{j,k}$ for large j can be ignored within a given tolerance ϵ. So we can dynamically adjust the number and locations of the collocation points used in the wavelet expansions, reducing significantly the cost of the scheme while providing enough resolution in the regions where the solution varies significantly. We can achieve this adaptivity in the following two ways.

5.4.1. Deleting collocation points. Let $\epsilon \ge 0$ be a prescribed tolerance and $j \ge 0$, $\ell = \ell(\epsilon) = \min(\frac{n_j}{2}, -\frac{\log \epsilon}{\log \alpha})$.

Step 1. First we locate the range for the index k,

$$\text{(5.6)} \qquad (k'_1, l'_1), \ldots, (k'_m, l'_m), \qquad m = m(j, \epsilon),$$

such that

$$\text{(5.7)} \qquad |\hat{u}_{j,k}| \le \epsilon, \qquad k'_i \le k \le l'_i,\ i = 1, \ldots, m.$$

Step 2. Following Theorems 3 and 4, we can ignore $\hat{u}_{j,k}$ in (5.2) for $k_i \le k \le l_i$, $i = 1, \ldots, m$, $k_i = k'_i + \ell + 3$, $l_i = l'_i - \ell - 3$, namely, we redefine $u_j(x)$ as

$$u_j(x) := \sum_{-1 \le k \le n_j - 2, k \in \mathcal{K}_j} \hat{u}_{j,k} \psi_{j,k}(x),$$

where $\mathcal{K}_j = \bigcup_{1 \le i \le m} [k_i, l_i]$.

Step 3. The new collocation points and unknowns will be

$$\{x_k^{(j)}\}, u_J(x_k^{(j)}), \qquad k = 1, \ldots, L-1, \text{ if } j = -1; k \in \{-1, \ldots, n_j - 2\} \backslash \mathcal{K}_j, \text{ if } j \ge 0.$$

5.4.2. Increasing level of wavelet space. Let $\epsilon \ge 0$ again be some prescribed tolerance, and if

$$\text{(5.8)} \qquad \max |\hat{u}^n_{J,k}| > \epsilon,$$

where subscript n indicates the solution at time $t = t^n$, then we can increase the number of wavelet spaces W_j in the expansion for the numerical solution $u_J(x)$ in (5.2), say, up to $W_{J'}$, $J' > J$.

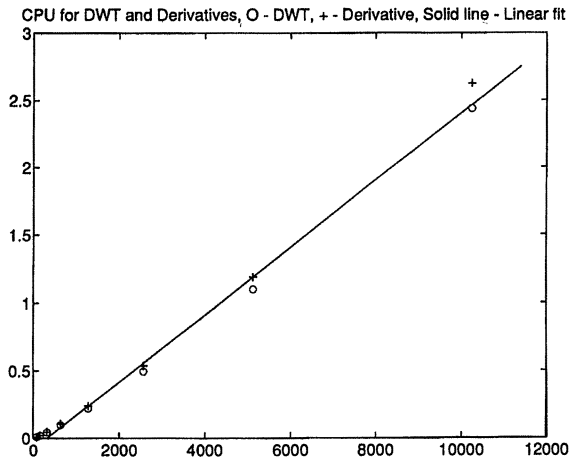

FIG. 5. *CPU timing for performing DWT transforms* (o) *(including both directions) and computation of the derivatives* (+). *The solid line shows a linear fitting of the data. Horizontal axis—number of unknowns; vertical axis—CPU time in seconds.*

Step 1. At $t = t^n$ if condition (5.8) is satisfied, let $J' > J$ and define a new solution vector

$$\tilde{\mathbf{u}}^n_{J'} := (\mathbf{u}^{(-1)}, \mathbf{u}^{(0)}, \ldots, \mathbf{u}^{(J-1)}, \mathbf{u}^{(J)}, \ldots, \mathbf{u}^{(J'-1)})^\top,$$

where for $J \le j \le J' - 1$, $\mathbf{u}^{(j)} = \{\mathcal{P}_J \mathbf{u}(x_k^{(j)})\}_{k=-1}^{n_j-2}$.

Step 2. Use $\tilde{\mathbf{u}}^n_{J'}$ on the right-hand side of scheme (5.5) to advance the solution to time step t^{n+1} and obtain solution $\mathbf{u}^{n+1}_{J'}$. Then, $u^{n+1}_{J'}(x) = \mathcal{P}_{J'} u^{n+1}_{J'} \in V_0 \oplus W_0 \oplus \cdots \oplus W_{J'-1}$ will be the new numerical solution which yields a better approximation of the exact solution of (5.1).

6. Numerical results.

6.1. CPU performance of DWT. The theoretical estimates of operations for performing the DWT in both directions and the computation of derivatives at all collocation points are $O(N \log N)$, where N is the total number of terms in the wavelet expansion (3.10).

We take the function in (6.1) and define its wavelet interpolation expansion (3.10) for $L = 10$, $J = 2, 3, \ldots, 10$; the total number of terms (or collocation points) $N = 2^J L - 1$ is between 79 and 10,240. In Figure 5, we plot the CPU time for the performance of DWT back and forth in both directions ("o" in the figure) and the computations of derivatives on all collocation points ("+" in the figure). Also drawn in the figure is a straight line which indicates an almost linear growth of the CPU timing up to 12,000 points.

6.2. Adaptive approximation of wavelet interpolation expansion. We consider a function with high gradients

$$f(x) = \begin{cases} h_1(x + 1, 0.3) & \text{if } -1 \le x \le -0.7, \\ 0 & \text{if } -0.7 \le x \le -0.5 - \delta, \\ h_1(x + 0.5, \delta) & \text{if } -0.5 - \delta \le x \le -0.5 + \delta, \\ 0 & \text{if } -0.5 + \delta \le x \le 0, \\ \sin(5\pi x) h_1(x - 0.25, 0.25) & \text{if } 0 \le x \le 0.5, \\ h_2(\frac{x-0.5}{2\delta}) & \text{if } 0.5 \le x \le 1, \end{cases} \tag{6.1}$$

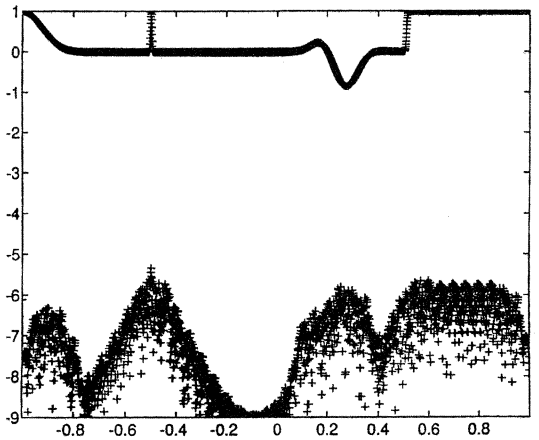

FIG. 6. *Wavelet approximation of functions* (6.1) *with* $L = 40$, $J = 6$. *Top—exact solution (solid line) and approximation* ("o"); *bottom—absolute error in logarithm scale. Total number of* $\hat{f}_{j,k}$ *is* 5123.

where $\delta = 0.01$, $h_1(x, a)$ is a hat function, and $h_2(x)$ is a step-like function and these functions are defined as

$$h_1(x,a) = \begin{cases} [\sin(\frac{\pi(x+a)}{2a})]^6 & \text{if } |x| < a, \\ 0 & \text{otherwise,} \end{cases} \tag{6.2}$$

and

$$h_2(x) = \begin{cases} 0 & \text{if } x < 0, \\ \frac{1}{2772}\int_0^x t^5(1-t)^5\,dt & \text{if } 0 \le x \le 1, \\ 1 & \text{otherwise.} \end{cases} \tag{6.3}$$

First, we construct the full wavelet interpolation expansion (3.10), i.e., $\mathcal{P}_J f(x)$, for $J = 7$, $L = 40$; the total number of wavelet functions (or the collocation points N) is $N + 4 = (2^J L - 1) + 4 = 2^J L + 3 = 5123$ (including four boundary functions in $\mathbf{I}_{b,J} f(x)$). At the top of Figure 6, we plot $f(x)$ (solid line) and $\mathcal{P}_J f(x)$ at non-interpolation points; at the bottom we have the absolute error in logarithmic scale. In Figure 7, we plot the components $f_0 \in V_0$ and $g_j(x) \in W_j$, $0 \le j \le 6$, in $\mathcal{P}_J f(x) = \mathbf{I}_{b,J} f(x) + f_0 + g_0 + \cdots + g_{J-1}$. We can see that only the higher frequency part is retained in higher wavelet spaces W_j (notice that the scale varies for different pictures).

Then, we use the procedure at the end of §5 to filter out the coefficients $\hat{f}_{j,k}$ which are less than ϵ in magnitude. In Figure 8, we take $\epsilon = 10^{-5}$ and the number of wavelet functions $\hat{f}_{j,k}$ reduces to 289 with the accuracy of the approximation (bottom curves) within order of ϵ. In Figure 9, we plot the solution at the remaining interpolation points and the expected clustering of the interpolation points is seen at locations where the function changes more dramatically. In Figure 10, we plot the magnitude of the wavelet coefficients $\hat{f}_{j,k}$, $j \ge -1$, one level above another. The high density of the wavelet coefficients reflects the existence of high gradients of the approximated function. In Figure 11, we take $\epsilon = 10^{-4}$ and the number of wavelet functions $\hat{f}_{j,k}$ reduces to 206 with the accuracy of the approximation (bottom curves) within order of ϵ.

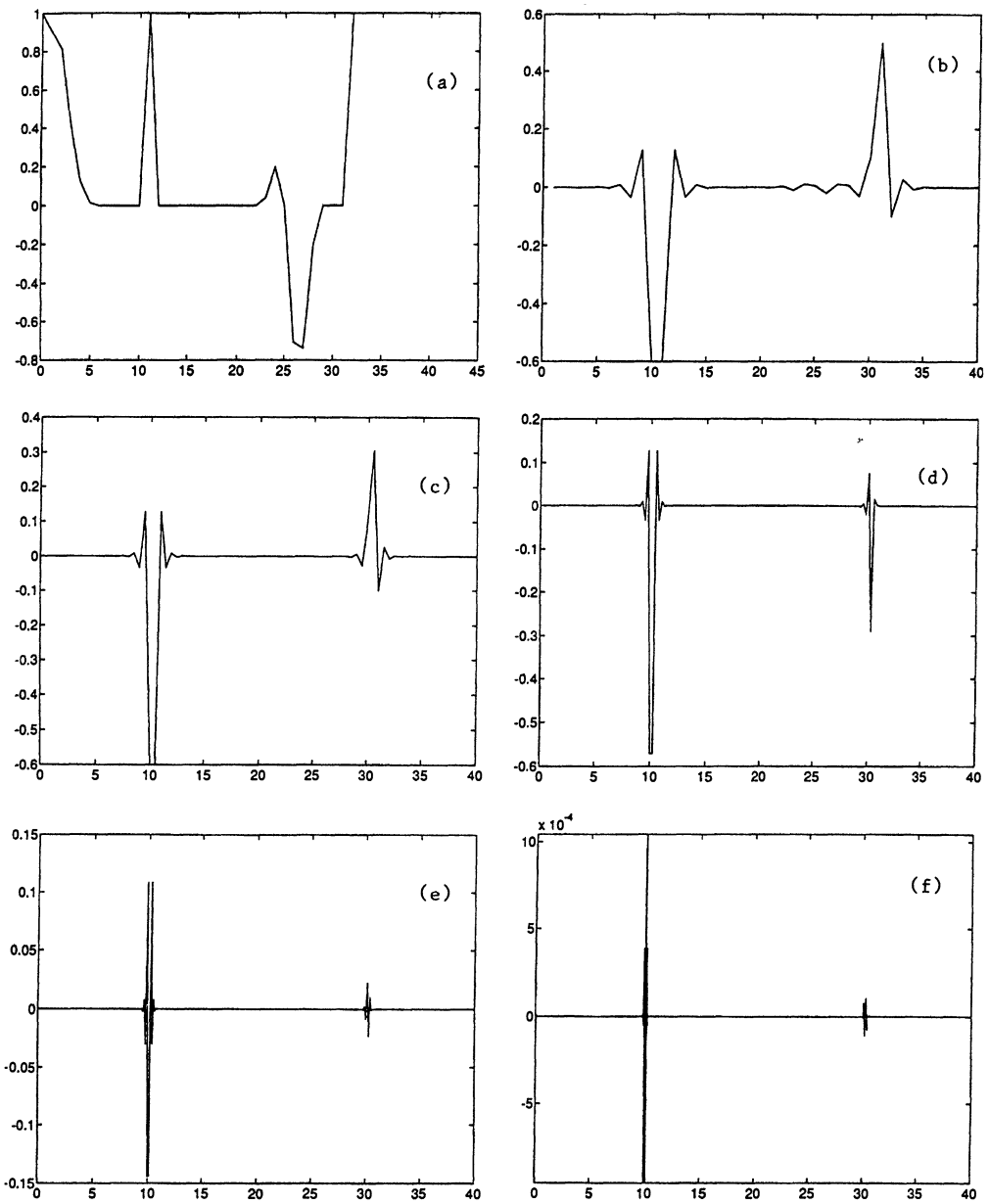

FIG. 7. *Components of* $\mathcal{P}_6 f(x) = f_0 + g_0 + \cdots + g_6$. *From top to bottom*—(a) f_0; (b) − (f) $g_0(x) - g_4(x)$. *Notice that the y-scales are different.*

6.3. Linear hyperbolic PDEs. We consider the problem of the linear hyperbolic PDE

$$\begin{cases} u_t + u_x = 0, & 0 \le x \le 1, \\ u(0,t) = 0, \\ u(x,0) = f(x) \text{ or } h_2(\frac{x}{2\delta}). \end{cases} \tag{6.4}$$

In Figure 12, we present the solution of (6.4) at $t = 0.1$ with initial condition $u(x,0) = h_2(\frac{x}{2\delta})$, $\delta = 0.004$, and the numerical parameter $L = 20$, $J = 8$, $\epsilon = 10^{-4}$. Third-order

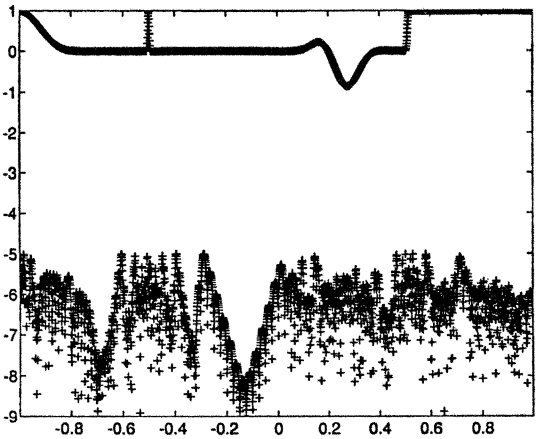

FIG. 8. *Same as Figure* 6 *but with deletion of wavelet coefficient* $\hat{f}_{j,k}$ *whose magnitude is less than* $\epsilon = 10^{-5}$. *Total number of* $\hat{f}_{j,k}$ *left is* 289.

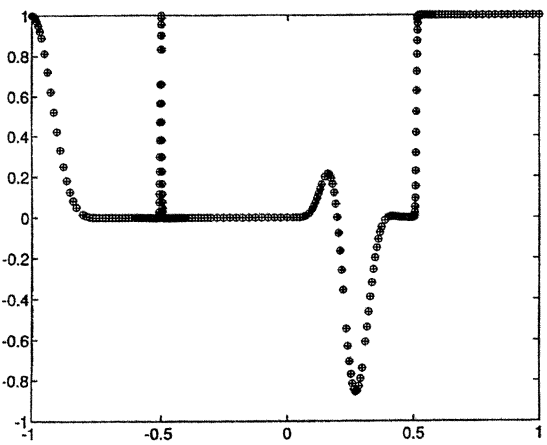

FIG. 9. *Close up of top part of Figure* 8, *numerical solutions* ("+") *at remaining collocation points against exact solutions* ("o").

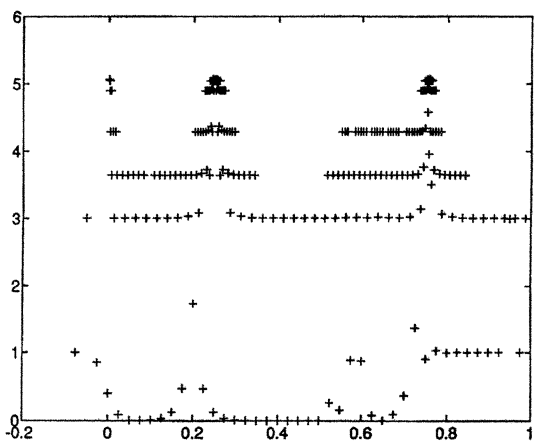

FIG. 10. *Magnitude of the wavelet coefficients in the approximation used in Figures* 8 *and* 9. *The coefficients are plotted so the coefficients in* W_{j+1} *are above those in* W_j.

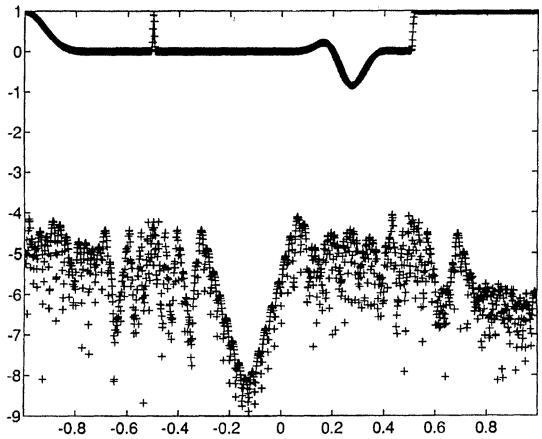

FIG. 11. *Same as Figure* 8 *but with* $\epsilon = 10^{-5}$. *Total number of* $\hat{f}_{j,k}$ *left is* 206.

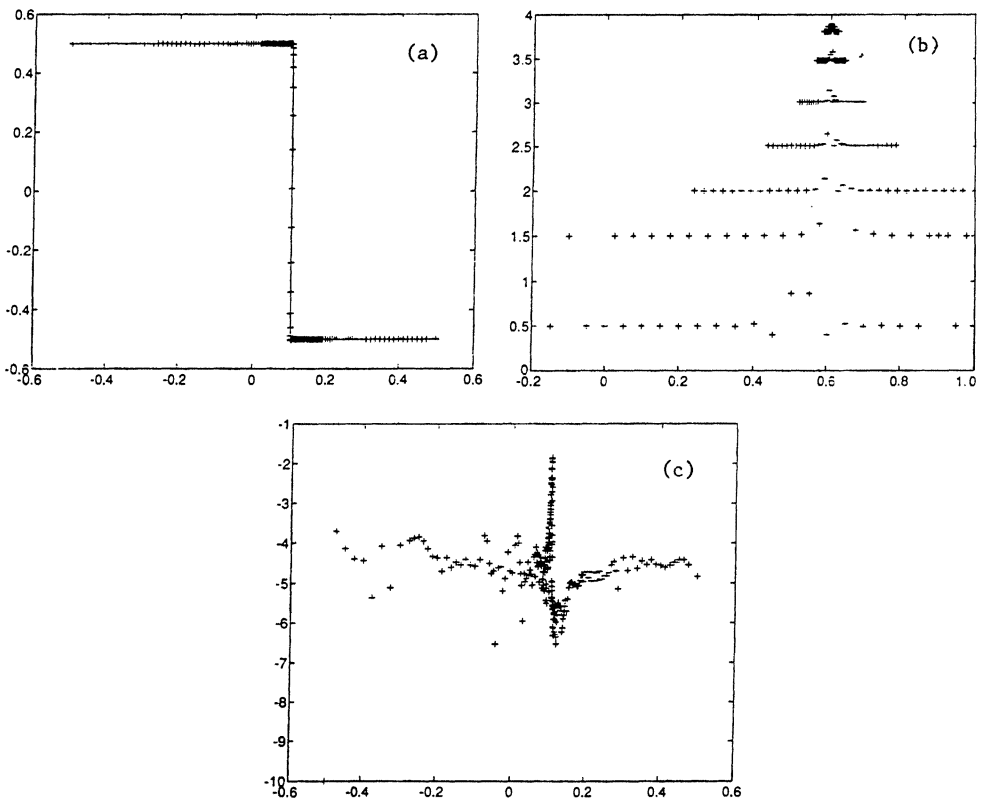

FIG. 12. *Adaptive wavelet collocation solution of linear PDE* (6.4) *with initial condition* (6.3) ($\delta = 0.004$) *at* $t = 0.1$ *with* $L = 20$, $J = 8$, *and error tolerance* $\epsilon = 10^{-4}$. *The number of collocation points* $N = 240$. (a) *plus sign—numerical solutions, solid line—exact solution*; (b) *wavelet coefficients at all levels*; (c) *errors at collocation points in logarithm scale.*

Runge-Kutta methods are used for all numerical results presented here. We update the mesh every five time steps. Figure 12(a) is the numerical solution (plus) at 240 collocation points at time $t = 0.1$ against the exact solution (solid line). Figure 12(b) shows the distribution of wavelet coefficients for each level of wavelet spaces. The number of collocation points

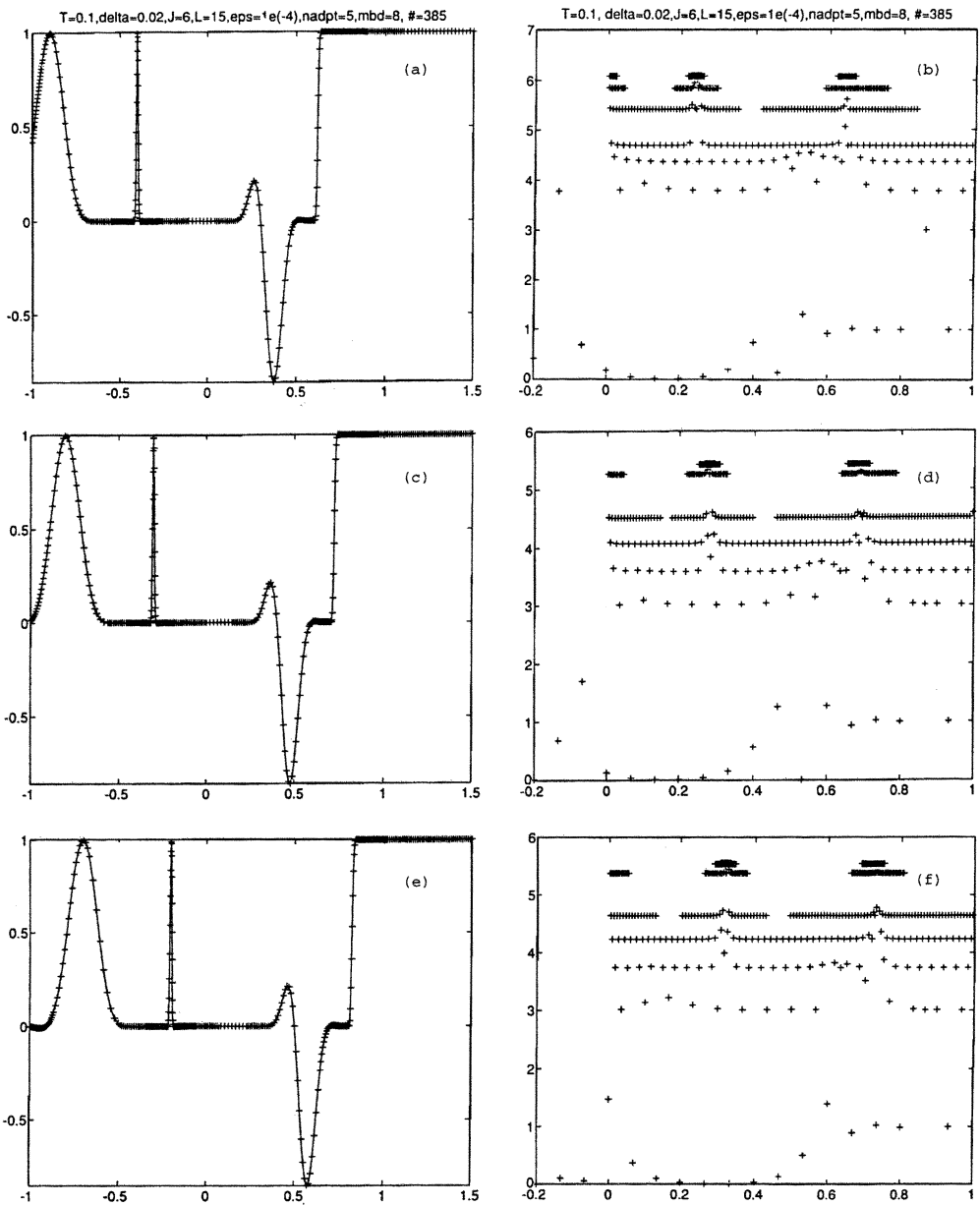

FIG. 13. *Adaptive wavelet collocation solution of linear PDE* (6.4) *with initial condition* (6.1) ($\delta = 0.02$) *at* $t = 0.1, 0.2, 0.3$ *with* $L = 15$, $J = 8$, *and error tolerance* $\epsilon = 10^{-4}$. *The number of collocation points* $N = 385, 394,$ *and* 392 *at time* $t = 0.1, 0.2,$ *and* 0.3, *respectively.* (a)-(c) *plus sign—numerical solutions, solid line—exact solution;* (d)-(f) *wavelet coefficients at all levels.*

fluctuates around 240 and only the wavelet coefficients of those wavelet basis functions close to the large gradients remained in the numerical solution. Figure 12(c) shows the errors of the numerical solution in logarithmic scale at all remaining collocation points.

Figures 13(a)-13(f) show the results of (6.4) with $f(x)$ in (6.1) as initial condition ($\delta = 0.02$) and the numerical parameters $L = 15$, $J = 7$, $\epsilon = 10^{-4}$. Figures 13(a)-13(c) show the solutions at time $t = 0.1, 0.2, 0.3$, when the number of collocation points is 385, 394, 392, respectively. Figures 13(d)-13(f) show the wavelet coefficients of the numerical solution at

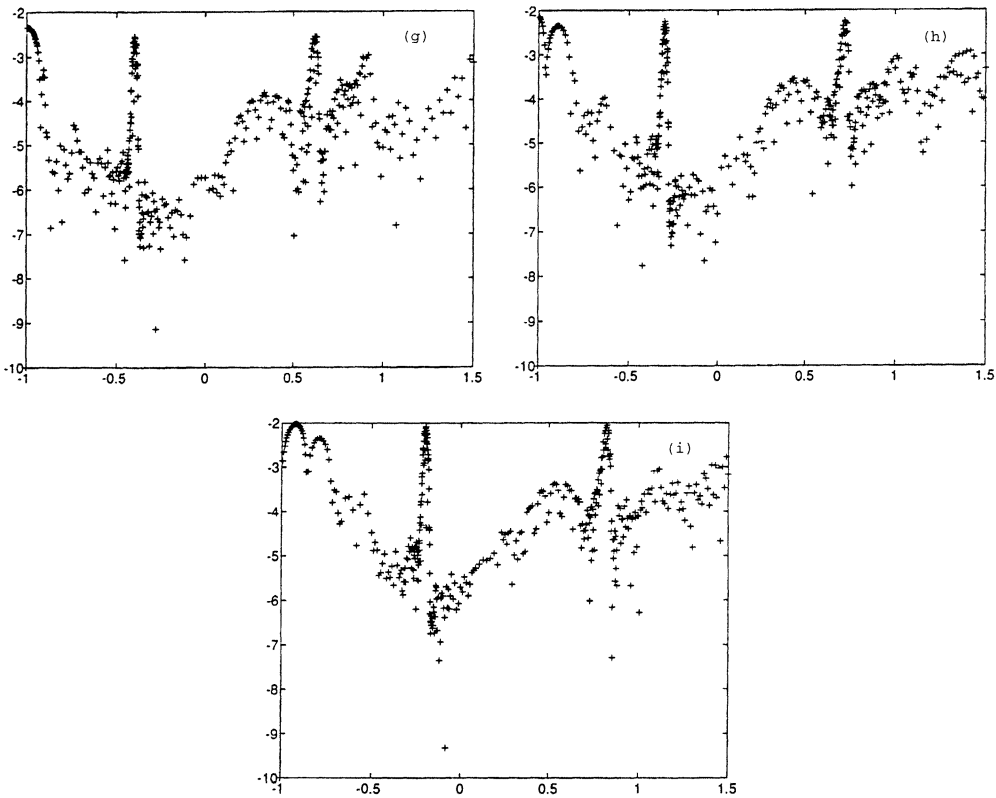

FIG. 13. (*cont.*). (g)-(i) *errors of numerical solutions in logarithm scale at* $t = 0.1, 0.2, 0.3$, *respectively.*

those times, i.e., $t = 0.1, 0.2$, and 0.3, respectively. Figures 13(g) and 13(i) show the errors of the numerical solutions in logarithmic scale at $t = 0.1, 0.2, 0.3$, respectively.

6.4. Inviscid Burger equation. Finally, we consider the problem of the nonlinear hyperbolic PDE

$$\begin{cases} u_t + (\frac{u^2}{2})_x = 0, & -1 \le x \le 2, \\ u(0,t) = \text{ given}, \\ u(x,0) = f(x), \end{cases} \tag{6.5}$$

where

$$f(x) = \begin{cases} -\sin(\pi x) & \text{if } -1 \le x \le 1, \\ 0 & \text{otherwise.} \end{cases} \tag{6.6}$$

The solution of Burger's equation develops a shock at time $t = \frac{1}{\pi} \sim 3.18$. In this case, we take $L = 15$, $J = 8$, $\epsilon = 10^{-4}$. With every five iterations we change the number and locations of the collocation points according to the criteria proposed at the end of §5. The number of collocation points is 292, 295, 303 at times $t = 0.3, 0.318, 0.319$, respectively, Figures 14(a)-14(c) show the numerical solutions at those three times, respectively, while Figure 14(d) shows the solution a little while after a shock has developed at location $x = 0$. Further integration of the solution after this time will produce oscillations in the numerical solution as the numerical method has no mechanism to capture a real shock. Again, Figures 14(d)-14(f) show the wavelet

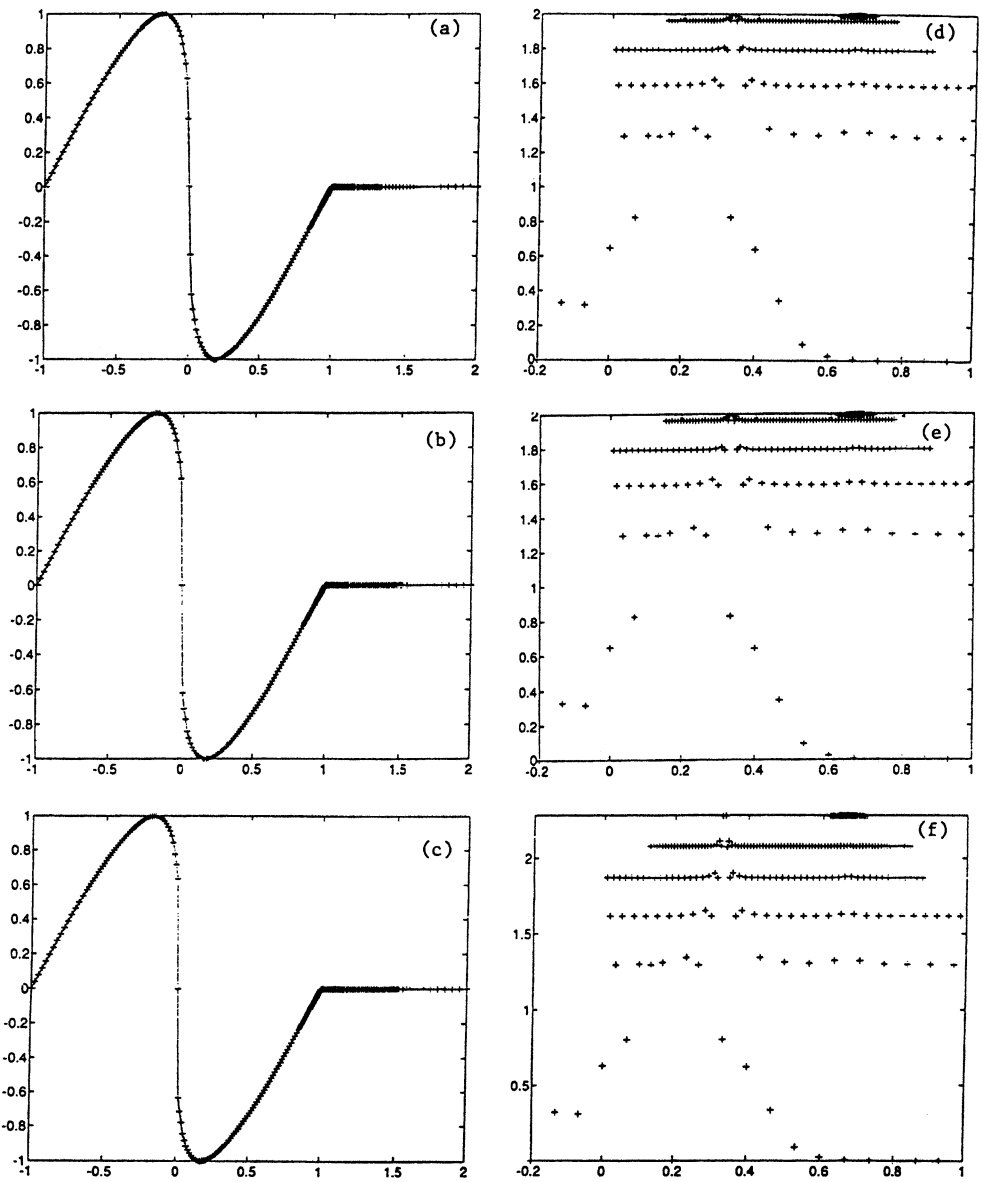

FIG. 14. *Adaptive wavelet collocation solution of inviscid Burger's equation* (6.5) *with initial condition* (6.6) *at* $t = 0.3, 0.318, 0.319$ *with* $L = 15$, $J = 8$, *and error tolerance* $\epsilon = 10^{-4}$. *The number of collocation points* $N = 292, 295,$ *and* 303 *at time* $t = 0.3, 0.318,$ *and* 0.319, *respectively.* (a)-(c) *plus sign—numerical solutions*; (d)-(f) *wavelet coefficients at all levels.*

coefficients used in the numerical solution at time $t = 0.30, 0.318$, and 0.319, respectively. The numerical scheme automatically puts more collocation points near the high gradient ($x = 0$) and the derivative discontinuity ($x = 1$). Again, the third-order Runge-Kutta methods are used for the time integration, whose stability is to be determined by the eigenvalue distribution of the first and second derivative matrices $\mathcal{D}_1$ and $\mathcal{D}_2$ shown in Figures 15 and 16, respectively.

7. Conclusion. In this paper, we have constructed a fast DWT which enables us to construct collocation methods for nonlinear PDEs. The adaptivity of wavelet approximation is conveniently implemented through the examination of the wavelet coefficients. The preliminary tests of the solution of PDEs indicate that such an approach will be important in

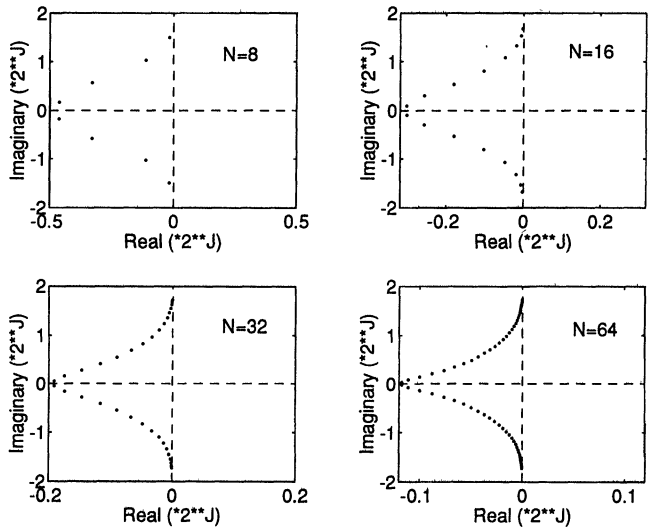

FIG. 15. *Eigenvalues for the first derivative matrix $\mathcal{D}_1$ for $L = 8$, $j = 0, 1, 2, 3$ whose sizes are 8, 16, 32, and 64, respectively.*

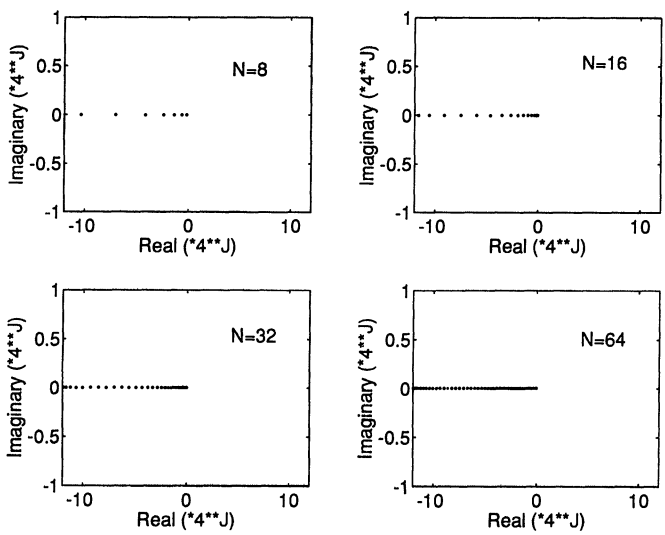

FIG. 16. *Eigenvalues for the second derivative matrix $\mathcal{D}_2$ for $L = 8$, $j = 0, 1, 2, 3$ whose sizes are 8, 16, 32, and 64, respectively.*

large-scale computations where the solution develops extremely high gradients in isolated regions and uniform mesh is not practical. A final note on the use of higher-order spline for the construction of MRA for Sobolev spaces: the method used in this paper can be utilized to yield higher-order approximation to smooth functions. Considering the compactness of the support of the wavelet functions and the required smoothness in solving second-order differential equations, we have limited our discussion to the case of cubic splines in this paper.

Appendix.

Proof of (3.29). The proof is a straightforward application of Lemma 6. For M_j in (3.9), we have $(a_2, a_3, \ldots, a_n) = (-\frac{1}{13}, -\frac{1}{14}, \ldots, -\frac{1}{14}, -\frac{1}{14})$, $(b_1, b_2, \ldots, b_n) = (1, 1, \ldots, 1)$, and $(c_2, c_3, \ldots, c_n) = (-\frac{1}{14}, -\frac{1}{14}, \ldots, -\frac{1}{14}, -\frac{1}{13})$, where $n = n_j = 2^j L$. Therefore, the

sequence $\{u_m\}$ in (3.26) satisfies the following relations:

$$u_0 = 0, \qquad u_1 = 1, \qquad u_2 = 14, \qquad u_3 = \frac{2534}{13}, \tag{A.1}$$

and for $4 \le m \le n$,

$$u_m = \bar{c}_m(-u_{m-2} + 14u_{m-1}), \tag{A.2}$$

where $\bar{c}_m = \frac{13}{14}$, if $m = n$; $\bar{c}_m = 1$, otherwise.

Recursive relation (A.2) is a finite difference of order 2 whose general solution is of the following form:

$$u_m = \bar{c}_m(c_1\alpha^{m-3} + c_2\beta^{m-3}), \tag{A.3}$$

where $\alpha = 7 + \sqrt{192}/2$, $\beta = 7 - \sqrt{192}/2$ are the two distinct roots of the quadratic equation

$$x^2 - 14x + 1 = 0,$$

and constants c_1 and c_2 are chosen so equation (A.3) is valid for $m = 2, 3$.

Therefore,

$$\begin{gathered} u_0 = 0, \qquad u_1 = 1, \\ u_m = \bar{c}_m(\mu_1\alpha^{m-3} + \mu_2\beta^{m-3}), \qquad 2 \le m \le n, \end{gathered} \tag{A.4}$$

where $\mu_1 = \frac{\alpha}{\alpha-\beta}(\frac{2534}{13} - 14\beta) > 0$, $\mu_2 = \frac{\beta}{\alpha-\beta}(14\alpha - \frac{2534}{13}) > 0$.

Similarly, we can show that

$$v_{n+1} = 0, \qquad v_n = 1, \tag{A.5}$$

$$v_m = \bar{c}_{n-m+1}(\mu_1\alpha^{n-2-m} + \mu_2\beta^{n-2-m}) \quad \text{for } 1 \le m \le n-1, \tag{A.6}$$

and

$$v_0 = -\frac{1}{a_1}(\delta_1\alpha^{n-4} + \delta_2\beta^{n-4}),$$

where $\delta_1 = \frac{(13\alpha-1)\mu_1}{14} > 0$, $\delta_2 = \frac{(13\beta-1)\mu_2}{14} < 0$.

Finally, following (3.28) in Lemma 5, we have the following estimates on the inverse of M_j.

Denote e_j, $1 \le j \le n$, as

$$e_j = \begin{cases} 1 & \text{if } j = 1, \\ \frac{13}{14} & \text{if } j = 2, \\ 1 & \text{if } 3 \le j \le n-1, \\ \frac{14}{13} & \text{if } j = n. \end{cases}$$

Case 1. $i \le j$ and $1 \le j \le n-1$, $i = 1$:

$$\alpha_{i,j} = -e_i\bar{c}_{n-j+1}\frac{(\mu_1\alpha^{n-2-j} + \mu_2\beta^{n-2-j})}{(\delta_1\alpha^{n-4} + \delta_2\beta^{n-4})}. \tag{A.7}$$

So we have

$$\begin{aligned}|\alpha_{i,j}| &\le \frac{14}{13}\frac{\alpha^{n-2-j}(\mu_1+\mu_2 z^{n-2-j})}{\alpha^{n-4}(\delta_1-\delta_2 z^{n-4})}\\ &\le \frac{14}{13}\frac{\alpha(\mu_1+\mu_2/z)}{(\delta_1-\delta_2)}\frac{1}{\alpha^{j-1}}\\ &= K_1\frac{1}{\alpha^{|j-i|}},\end{aligned}$$

where $z=\frac{\beta}{\alpha}\le 1$ and $K_1 \doteq 1.1666$.

Case 2. $i \le j$ and $1 \le j \le n-1, 2 \le i \le n$:

$$\alpha_{i,j} = -e_i\bar{c}_{n-j+1}\bar{c}_i\frac{(\mu_1\alpha^{i-3}+\mu_2\beta^{i-3})(\mu_1\alpha^{n-2-j}+\mu_2\beta^{n-2-j})}{(\delta_1\alpha^{n-4}+\delta_2\beta^{n-4})}. \tag{A.8}$$

Case 3. $i \le j$ and $j = n, i = 1$:

$$\alpha_{i,j} = -e_i\frac{1}{(\delta_1\alpha^{n-4}+\delta_2\beta^{n-4})}. \tag{A.9}$$

Case 4. $i \le j$ and $j = n, 2 \le i \le n$:

$$\alpha_{i,j} = -e_i\bar{c}_i\frac{(\mu_1\alpha^{i-3}+\mu_2\beta^{i-3})}{(\delta_1\alpha^{n-4}+\delta_2\beta^{n-4})}. \tag{A.10}$$

Case 5. $i > j$ and $j = 1, 1 \le i \le n-1$:

$$\alpha_{i,j} = -e_j\bar{c}_{n-i+1}\frac{\mu_1\alpha^{n-2-i}+\mu_2\beta^{n-2-i}}{(\delta_1\alpha^{n-4}+\delta_2\beta^{n-4})}. \tag{A.11}$$

Case 6. $i > j$ and $j = 1, i = n$:

$$\alpha_{i,j} = -e_j\frac{1}{(\delta_1\alpha^{n-4}+\delta_2\beta^{n-4})}. \tag{A.12}$$

Case 7. $i > j$ and $2 \le j \le n-1, 1 \le i \le n-1$:

$$\alpha_{i,j} = -e_j\bar{c}_j\bar{c}_{n-i+1}\frac{(\mu_1\alpha^{j-3}+\mu_2\beta^{j-3})(\mu_1\alpha^{n-2-i}+\mu_2\beta^{n-2-i})}{(\delta_1\alpha^{n-4}+\delta_2\beta^{n-4})}. \tag{A.13}$$

Case 8. $i > j$ and $2 \le j \le n-1, i = n$:

$$\alpha_{i,j} = -e_j\frac{(\mu_1\alpha^{j-3}+\mu_2\beta^{j-3})}{(\delta_1\alpha^{n-4}+\delta_2\beta^{n-4})}. \tag{A.14}$$

For Cases 2–8, we can similarly obtain

$$|\alpha_{i,j}| \le \frac{K_i}{\alpha^{|j-i|}}, \qquad 2 \le i \le 8,$$

where $K_2 \doteq 1.1726$, $K_3 \doteq 1.1607$, $K_4 \doteq 1.1666$, $K_5 \doteq 1.1666$, $K_6 \doteq 1.1607$, $K_7 \doteq 1.1722$, and $K_8 \doteq 1.1666$.

Finally, if we choose $K = 1.1726$, then

$$|\alpha_{i,j}| \le \frac{K}{\alpha^{|j-i|}}, \qquad 1 \le i, j \le n. \tag{A.15}$$

This concludes the proof. □

Acknowledgments. The authors would like to thank the editor and, especially, the reviewers of this paper for their suggestions.

REFERENCES

[1] R. GLOWINSKI, A. RIEDER, R. O. WELLS, JR., AND X. ZHOU, *A Wavelet Multilevel Method for Dirichlet Boundary Value Problems in General Domains*, Technical Report 93-06, Computational Mathematics Laboratory, Rice University, 1993.

[2] E. BACRY, S. MALLAT, AND G. PAPANICOLAOU, *A Wavelet Based Space-Time Adaptive Numerical Method for Partial Differential Equations*, Technical Report No. 591, Robotics Report No. 257, Courant Institute of Mathematical Sciences, New York University, New York, NY, 1991.

[3] G. BEYLKIN, *On Wavelet-Based Algorithm for Solving Differential Equations*, Department of Mathematics, University of Colorado, 1992, preprint.

[4] L. GREENGARD AND V. ROKHLIN, *On the Numerical Solution of Two-Point Boundary Value Problems*, Technical Report, YALEU/DCS/RR-692, Yale University, New Haven, CT, 1989.

[5] S. JAFFARD, *Wavelet methods for fast resolution of elliptic problems*, SIAM J. Numer. Anal., 29 (1992), pp. 965-986.

[6] J.-C. XU AND W.-C. SHANN, *Galerkin-wavelet methods for two point boundary value problems*, Numer. Math., 63 (1992), pp. 123-142.

[7] I. DAUBECHIES, *Orthogonal bases of compactly supported wavelets*, Comm. Pure Appl. Math., 41 (1988), pp. 909-996.

[8] Y. MEYER, *Ondelettes ét opétateurs*, I: *Ondelettes*, Hermann, Paris, 1990.

[9] C. K. CHUI, *An Introduction to Wavelets*, Academic Press, New York, San Diego, 1992.

[10] A. COHEN, I. DAUBECHIES, AND P. VIAL, *Wavelets on the interval and fast wavelet transforms*, Appl. Comput. Harmonic Anal., 1 (1993), pp. 54-81.

[11] Y. MEYER, *Ondelettes sur l'intervalle*, Rev. Mat. Iberoamericana, 7 (1991), pp. 115-143.

[12] C. K. CHUI AND E. QUAK, *Wavelets on a Bounded Interval*, CAT Report 265, Department of Mathematics, Texas A & M University, College Station, TX, 1992.

[13] A. HARTEN, *Multiresolution Representation of Data*, Courant Mathematics and Computing Laboratory Report No. 93-002, New York University, New York, NY, 1993.

[14] J. Z. WANG, *Cubic spline wavelet bases of Sobolev spaces and multilevel interpolation*, Appl. Comput. Harmonic Anal., 3 (1996), to appear.

[15] G. BEYLKIN, R. COIFMAN, AND V. ROKHLIN, *Fast wavelet transforms and numerical algorithms* I, Comm. Pure Appl. Math., 44 (1991), pp. 141-183.

[16] R. ADAMS, *Sobolev Spaces*, Academic Press, New York, San Diego, 1975.

[17] I. J. SCHEONBERG, *Cardinal Spline Interpolation*, in CBMS-NSF Series in Applied Math 12, Society for Industrial and Applied Mathematics, Philadelphia, PA, 1973.

[18] C. A. HALL AND W. W. MERYER, *Optimal error bounds for cubic spline interpolation*, J. Approx. Theory, 16 (1976), pp. 105-122.

[19] T. R. LUCAS, *Error bounds for interpolating cubic splines under various end conditions*, SIAM J. Numer. Anal., 11 (1974), pp. 569-584.

[20] C. R. DE BOOR, *A Practical Guide to Splines*, Springer-Verlag, New York, 1978.

[21] B. K. SWARTZ AND R. S. VARGA, *Error bounds for spline and L-spline interpolation*, J. Approx. Theory, 6 (1972), pp. 6-49.

[22] H. YSERENTANT, *On the multi-level splitting of finite elment spaces*, Numer. Math., 49 (1986), pp. 379-412.

[23] S. JAFFARD AND PH. LAURENCOT, *Orthogonal wavelets, analysis of operators, and applications to numerical analysis*, in Wavelets—A Tutorial in Theory and Applications, C.K. Chui, ed., Academic Press, New York, San Diego, 1992, pp. 542-601.

[24] Y. IKEBE, *On the inverse of band matrix*, Linear Algebra Appl., 24 (1979) pp. 93-97.

[25] W. CAI AND C. W. SHU, *Uniform high order spectral methods for one and two dimensional Euler equations*, J. Comput. Phys., 104 (1993), pp. 427-443.

[26] L. JAMESON, *On the Differential Matrix for Daubechies-based Wavelets on an Interval*, ICASE Report 93-94, Langley Research Center, Hampton, VA, 1993.